

## **Reply to the Comments of the Referee #1**

### **General Comments:**

**1. The title was “Projected Changes in Haze Pollution Potential in China”, but what were analyzed were the AEC and WVD. Thus, the quantized relationships between haze pollution (days) and AEC, WVD should be proved and illustrated. That is, why the AEC and WVD could be used to represent the haze?**

*Reply:* As mentioned in the manuscript, the AEC, which is associated with the wet deposition and the ventilation, provides a direct way to investigate the change of the haze pollution potential, and has been applied in the operational work for the forecasting of pollution potential in China Meteorological Administration (CMA). According to previous studies, high (low) AEC is disadvantageous (advantageous) for the occurrence of haze pollution; longer (shorter) WVD corresponds to more (less) haze pollution incidents. This is the theory foundation for the relationships between haze days and AEC, WVD.

In respond to the comment, we carried out further analysis to verify the relationships of the haze days with the AEC and the WVD. The observed data of haze days, which are based on daily visibility and relative humidity records from ~2400 observation stations in China, are provided by the CMA. The occurrence of a haze day is defined with the criteria: 1) daily mean visibility below 10 km; 2) daily mean relative humidity less than 90%. Because the visibility data were collected in different forms before and after 1980 caused by different observational rules, the period 1980-2016 is used for analysis. As shown in Fig. S1, the haze mainly occurs in eastern China, particularly in the Beijing-Tianjin-Hebei region, the Yangtze River Delta, the Pearl River Delta, and Northeast China.

Correlations between annual haze days and AEC, WVD are calculated over each station. It shows that there are negative correlations between the haze days and the AEC, and positive correlations between the haze days and the WVD over most of stations, especially in eastern China where the haze mainly occurs (Figs. S2, S3).

Considering large uncertainties from emission sources and complex chemical process for the haze genesis, the relationships between haze days and AEC, WVD are quite robust and strong. The related analysis have been added in section 2.2.

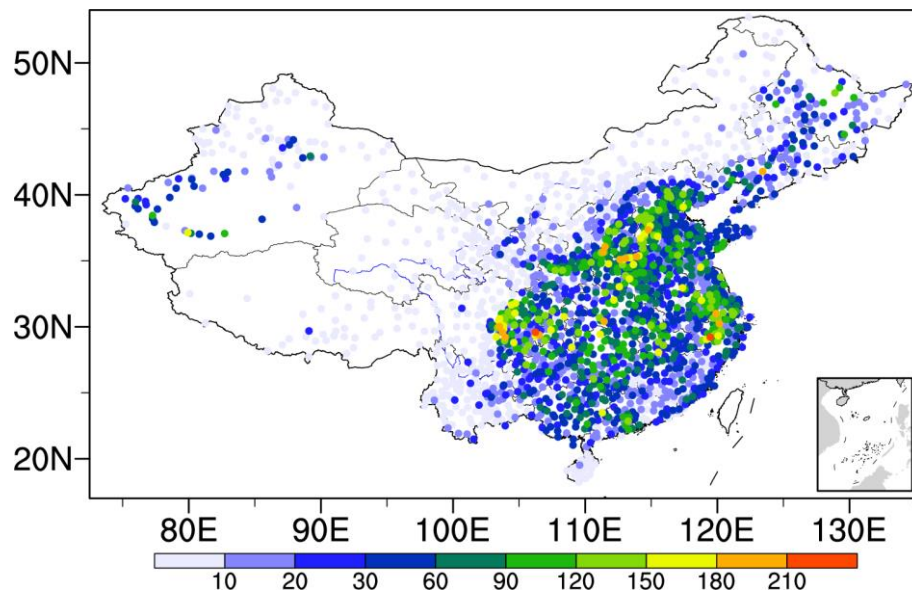


Fig. S1. Distribution of the averaged annual haze days over China during 1980-2016

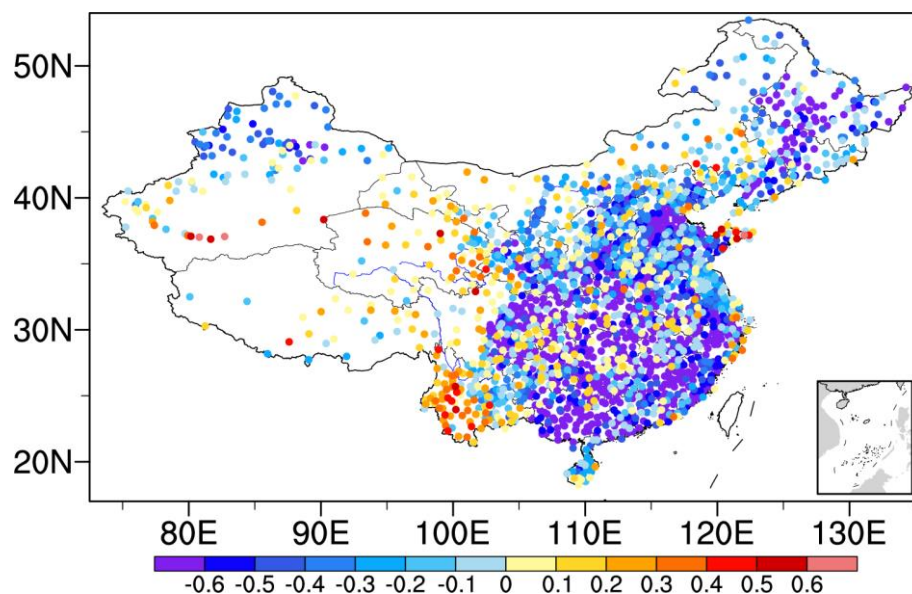


Fig. S2. Distribution of correlation coefficient between annual haze days and AEC

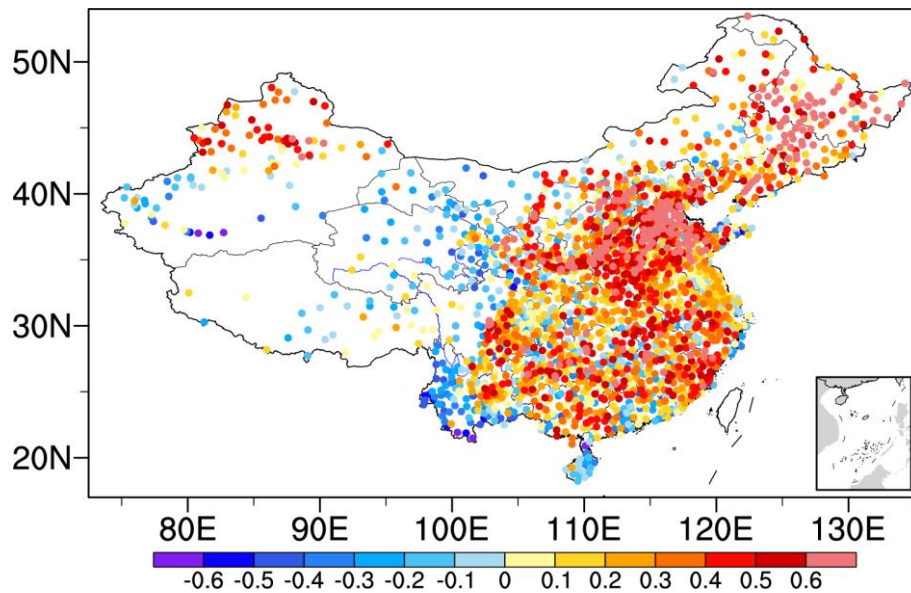


Fig. S3. Distribution of correlation coefficient between annual haze days and WVD

**2. According to prior studies, the relative humidity was vital for the incident of haze. If you want to evaluate the haze pollution potential, the moisture conditions must be considered.**

*Reply:* What we focus on in this study is the atmospheric carrying capacity, which is only related to the wet deposition and the ventilation. The relative humidity does be an important factor affecting the incident of haze. However, it is beyond the scope of this study. In the manuscript, we added a short discussion to clarify this issue in the last paragraph.

**3. “If each of the 6-hourly ventilation coefficients within one day is less than 6000  $\text{m}^2 \text{s}^{-1}$ , this day is counted as one weak ventilation day (WVD)”. The threshold was cited from (Leung and Gustafson, 2005), a study of U.S. air quality, and was actually and firstly used by Pielke et al (1991). The question was that if the same threshold was reasonable for the recent haze pollution in China.**

**Pielke, R. A., R. A. Stocker, R. W. Arritt, and R. T. McNider (1991), A procedure to estimate worst-case air quality in complex terrain, *Environ. Int.*, 17, 559– 574.**

*Reply:* The threshold is just used to indicate the intensity of ventilation, similar to that

for precipitation or wind. The effect of ventilation on air pollutant may not change among different places. Thus, the value of less than  $6000 \text{ m}^2 \text{ s}^{-1}$  for ventilation coefficient was used not only in the U.S. (Leung and Gustafson, 2005; Trail et al., 2013), but also in other places such as India (Goyal and Rao, 2007; Manju et al., 2002), Athens (Kassomenos et al., 1995), and Thailand (Pimonsree, 2008).

Further, we conducted a sensitivity analysis to examine the relationships between WVD and haze days when different thresholds (3000, 5000, 6000, 7000, and 9000  $\text{m}^2 \text{ s}^{-1}$ ) are used for the calculation of WVD. The result shows little change in their relationship under different thresholds (Fig. S4). Therefore, the threshold is reasonable for the analysis of this study.

Related clarification has been added in the second paragraph of section 2.2.

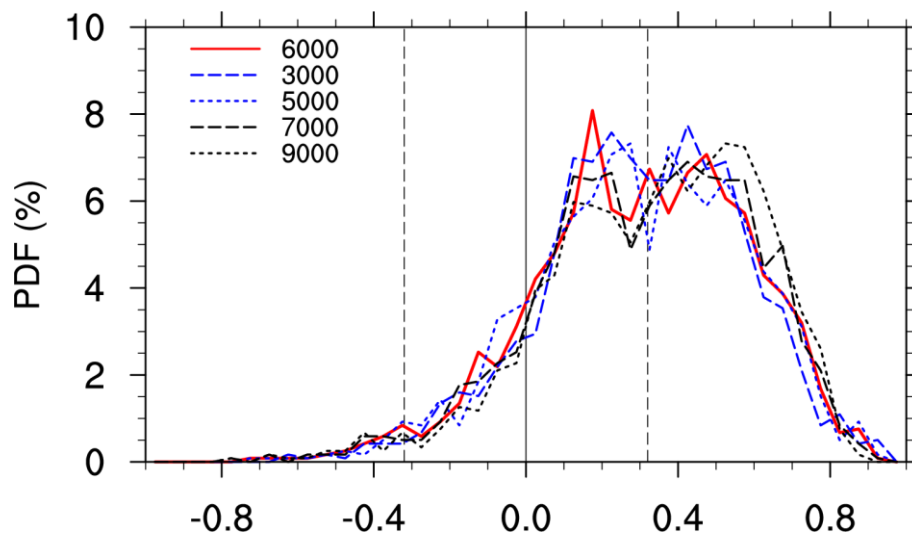


Fig. S4. Probability density function on the distribution of correlation coefficient between annual haze days and WVD. Different thresholds are used for the WVD calculation. Two dash lines indicate the 95% confidence level

Goyal, S., and Rao, C. C.: Air assimilative capacity-based environment friendly siting of new industries—A case study of Kochi region, India, *J. Environ. Manage.*, 84, 473-483, 2007.

Kassomenos, P., Kotroni, V., and Kallos, G.: Analysis of climatological and air quality observations from greater Athens area, *Atmos. Environ.*, 29, 3671-3688, 1995.

Manju, N., Balakrishnan, R., and Mani, N.: Assimilative capacity and pollutant

dispersion studies for the industrial zone of Manali, Atmos. Environ., 36, 3461-3471, 2002.

Pimonsree, S.: PM10 dispersion during air pollution episode in Saraburi, Thailand, Asia-Pacific Journal of Science and Technology, 13, 1185-1190, 2008.

Trail, M., Tsimpidi, A., Liu, P., Tsigaridis, K., Hu, Y., Nenes, A., and Russell, A.: Downscaling a global climate model to simulate climate change over the US and the implication on regional and urban air quality, Geoscientific Model Development, 6, 1429, 2013.

**4. The recent winter haze pollution in North China or BTH area was severest, but the bias of historical estimations in winter and in North China was very significant. Thus, the error bars or confidence intervals must be discussed.**

*Reply:* Similar to the contribution analysis in section 5, we applied the same method to investigate the contribution of different factors to the simulated AEC biases (Fig. S6). Overall, the simulation bias in boundary layer depth is the major factor for the simulated AEC bias over most parts of China (Fig. S6d). The related discuss is added in the first paragraph of section 3.

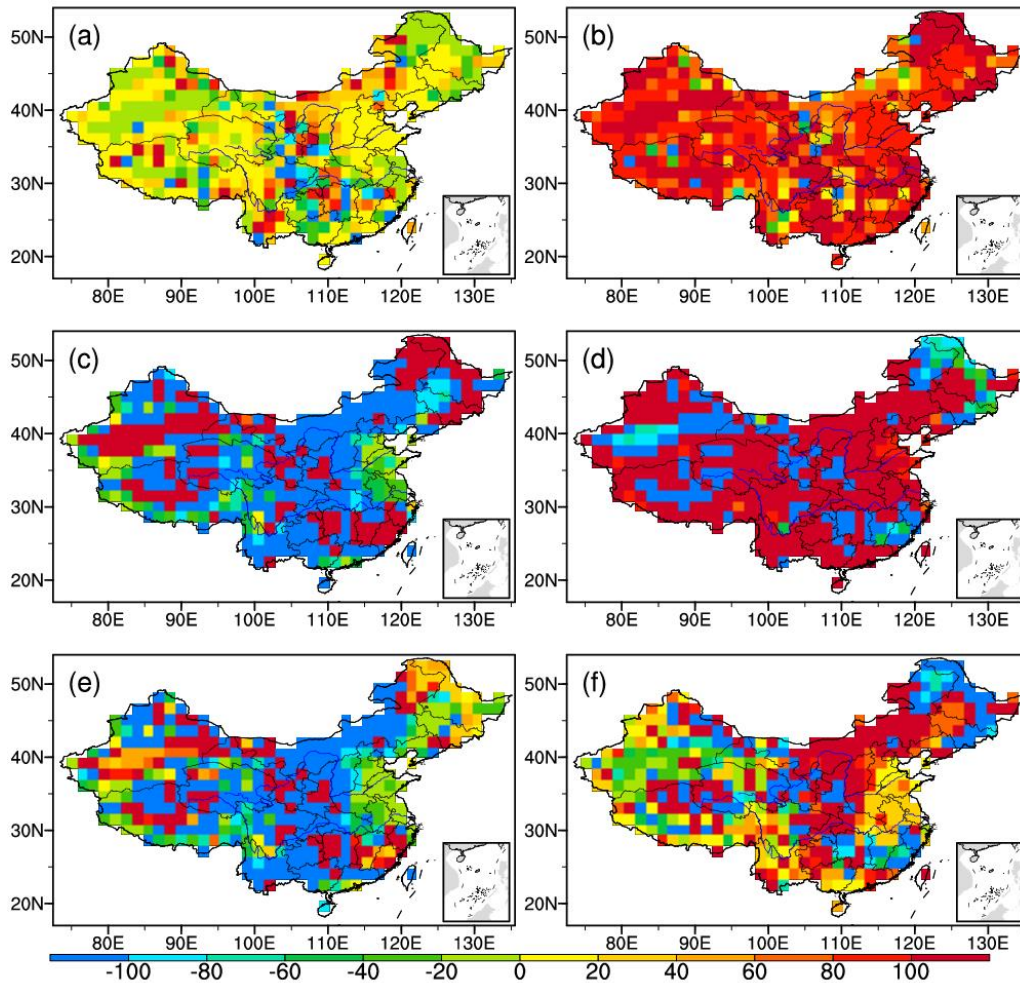


Fig. S5. Relative contributions (unit: %) of individual components to annual AEC biases based on the ensemble results. (a) precipitation, (b) ventilation, (c) wind speed averaged with the boundary layer, (d) boundary layer depth, (e) nonlinear term, (f) transient term.

#### Specific Comments:

**1. As well known, there were dozens of models in the CMIP5 project, so the reasons why only three models were selected should be supplemented. Furthermore, why did the authors only analyze two periods, i.e., 2046-2065 and 2080-2099?**

*Reply:* In CMIP5, ~20 GCMs provide the six-hourly outputs of wind speed, temperature, and humidity for dynamical downscaling. However, to drive RCM



modeling, the ratio of the resolution between GCMs and RCMs should not exceed 6-8. So, only those GCMs with the resolution of 1~2 degree can be used to drive RegCM4 simulations. Due to the availability of CMIP5 GCMs and considering large volume of outputs for ~120-yr RegCM4 simulations, we just used these three GCMs for this study. This part has been added in section 2.1.

The periods 2046-2065 and 2080-2099 are commonly used to represent near-term and long-term in the CMIP5 projection, respectively (IPCC, 2013). This has been clarified in the first paragraph of section 4

**2. The definition of Beijing-Tianjin-Hebei region (BTH), Northeast China (NEC), Yangtze River Delta economic zone (YRD), and Pearl River Delta economic zone (PRD) must be illustrated clearly.**

*Reply:* A map has been added in the revised manuscript (Fig. S6, also see Fig. 1f in the manuscript).

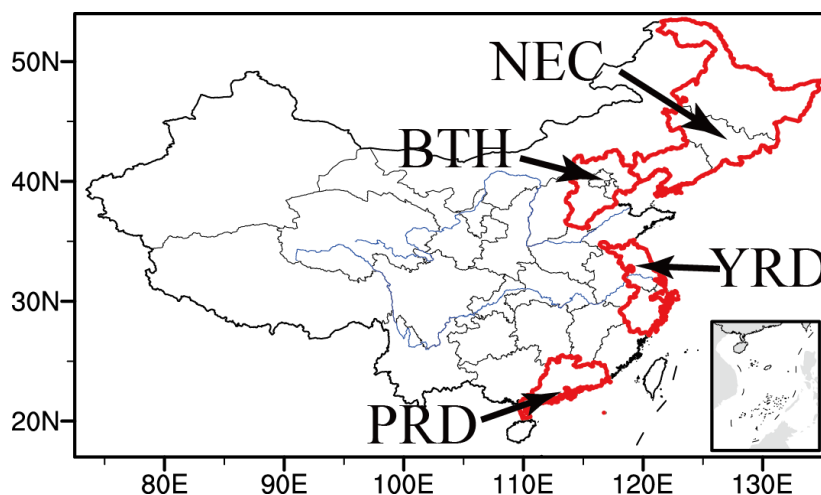


Figure S6. Four main economic zones of China, Beijing-Tianjin-Hebei region (BTH), Northeast China (NEC), Yangtze River Delta economic zone (YRD), and Pearl River Delta economic zone (PRD)

**3. In Figure 1–3, the resolutions of the observations was bad for evaluating the performance of Regcm4 downscaling. I noticed that the Era-interim used here was with the resolution 1.5\*1.5°, and suggest that the data 0.5\*0.5° should be**

**better.**

*Reply:* The native horizontal spatial resolution for the ERA-interim data is a T255 Gaussian grid, equivalent to a horizontal resolution of about 79 km or  $0.75^{\circ}$ . The data with other resolutions are bilinear interpolated from the native Gaussian grid (<https://software.ecmwf.int/wiki/display/CKB/>). So in the revised manuscript,  $0.75^{\circ}$  \* $0.75^{\circ}$  grid data are used. The conclusions for the evaluation are not changed (see Table 1, Table 2 and the figures for the observation in the manuscript).



## **Reply to the Comments of the Referee #2**

**1. My main criticism of this study is that the authors did not consider the impacts of reduced emissions in the future under RCP4.5 scenario on pollution risk. The haze pollution risk should relate to the aerosol concentrations. For example, higher background concentration lead a higher pollution risk with the same AEC. Thus, a discussion about how the pollution risk changed due to changes in emission is at least needed.**

*Reply:* As pointed out by the Referee, the haze pollution risk does be related to the aerosol concentrations. However, what we discussed here focused on the atmospheric carrying capacity which is associated with wet deposition and ventilation and provides a condition to transport and dilute pollutants. It does not reflect real emission characteristics. Since there is no chemistry/aerosol module coupled in our experiments, the contribution of emissions to pollution change under RCP4.5 scenario cannot be calculated. In responding to the comment, we added a short discussion to address it in the manuscript (see the last paragraph).

**2. Line 124- In the equation (1), how could authors distinguish the intensity of rainfall? The wet deposition with 10 mm/hour (and no precipitation in other 23 hours) should be different with 10 mm/24 hour.**

*Reply:* We used 6-hourly data for the AEC calculation, so short-duration (no longer than 6 hours) and long-duration events can be roughly distinguished. Due to large volume of the outputs from ~120-yr simulations by regional climate model, the time resolution of the model output is limited especially for those 3D variables (e.g. geopotential height, wind speed).

**3. Line 175-176 Why the AEC is underestimated over the southern Xinjiang and overestimated over parts of North China? Which one is the major reason? Simulated precipitation, wind speed, or boundary layer depth?**

*Reply:* Similar to the contribution analysis in section 5, we applied the same method to investigate the contribution of different factors to the simulated AEC biases (Fig. S1). Overall, the simulation bias in boundary layer depth is the major factor for the simulated AEC bias over most parts of China (Fig. S1d). The related discuss is added in the first paragraph of section 3.

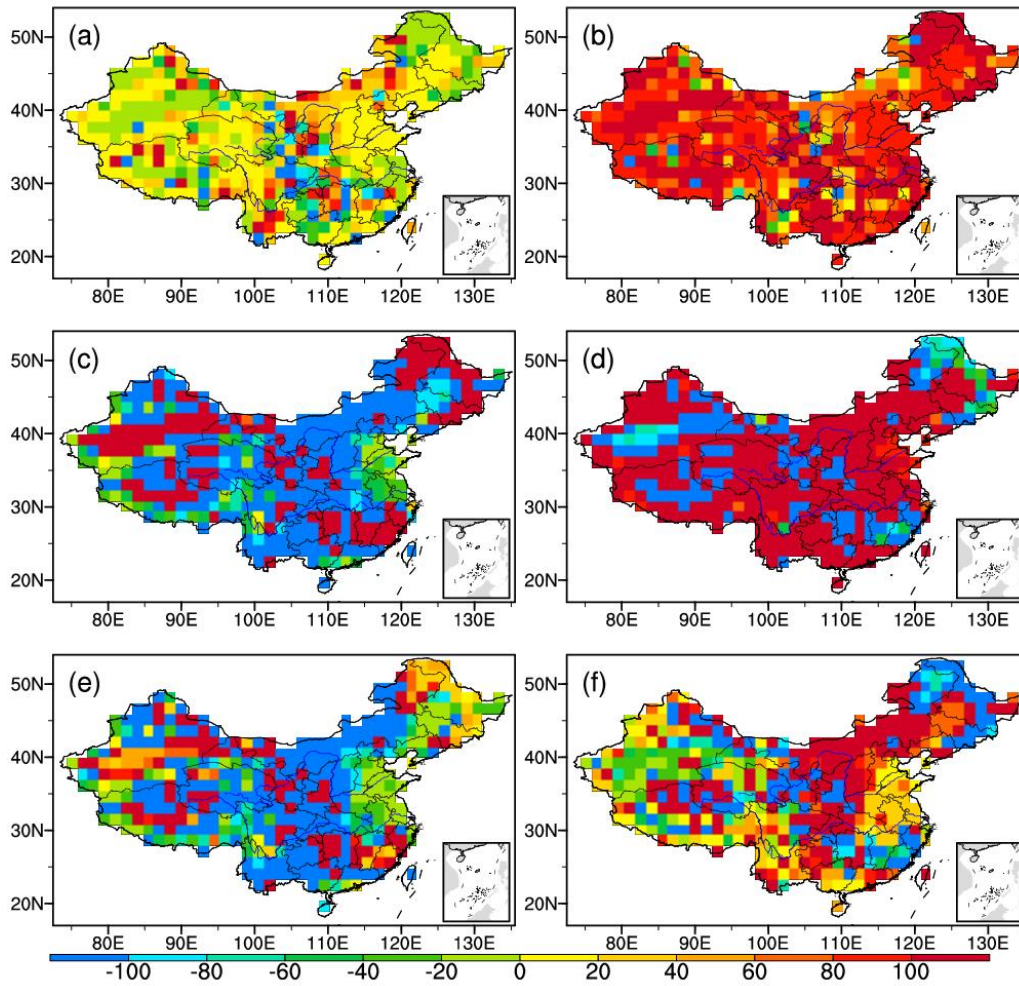


Figure S1. Relative contributions (unit: %) of individual components to annual AEC biases based on the ensemble results. (a) precipitation, (b) ventilation, (c) wind speed averaged with the boundary layer, (d) boundary layer depth, (e) nonlinear term, (f) transient term.

**4. Line 217- “Southwest China, northern North China, Northeast China: :” A map is needed.**

*Reply:* A map has been added in the revised manuscript (Fig. S2, also see Fig. 1f in

the manuscript).

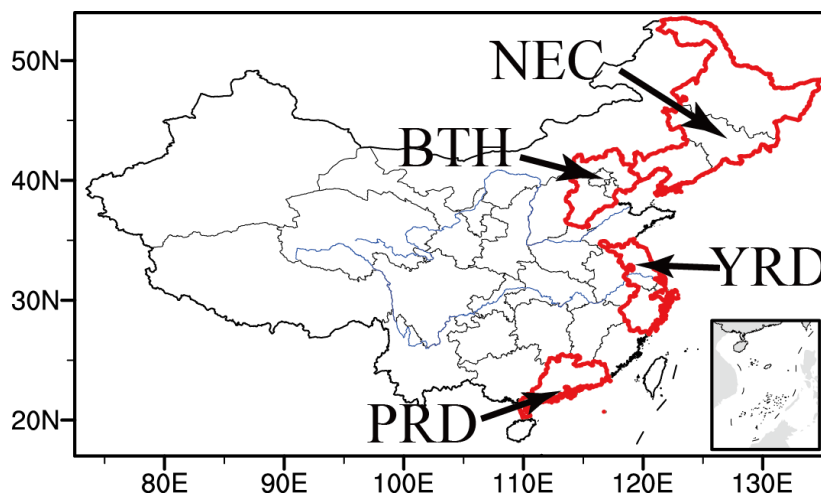


Figure S2. Four main economic zones of China, Beijing-Tianjin-Hebei region (BTH), Northeast China (NEC), Yangtze River Delta economic zone (YRD), and Pearl River Delta economic zone (PRD)

**5. Line-304-306. Missing WVD bar in Fig.7b in JJA during the middle of the 21<sup>st</sup> century.**

*Reply:* The percentage change of WVD in JJA during the middle of the 21<sup>st</sup> century is very small (0.008%), so the bar looks “missing”.

**6. Line 364- Change “dominant” to “important”. I don’t think the annual 20%-30% could described as “dominate role”.**

*Reply:* Changed.

**7. Line 392-400. In addition to the wind speed and boundary layer depth, will the wind direction change in the future? Does it also have impact on the air environment carrying capacity and haze pollution potential?**

*Reply:* As mentioned above, what we concerned in this study is the atmospheric carrying capacity that is only related to wet deposition and ventilation. The change of wind direction should be important. For example, the pollution from upwind emission sources could impact the air quality in some locations downwind. The wind direction

may also change in the future. However, this topic is beyond the scope of this study. A short discussion has been added to clarify this issue in the manuscript (see the last paragraph in section 5).

1       **Projected Changes in Haze Pollution Potential in China: An**  
2               **Ensemble of Regional Climate Model Simulations**

3  
4               Zhenyu Han<sup>1</sup>, Botao Zhou<sup>1,2</sup>, Ying Xu<sup>1</sup>, Jia Wu<sup>1</sup>, Ying Shi<sup>1</sup>

5       <sup>1</sup> National Climate Center, China Meteorological Administration, Beijing, China

6       <sup>2</sup> Collaborative Innovation Center on Forecast and Evaluation of Meteorological  
7       Disasters, Nanjing University of Information Science & Technology, Nanjing, China

8  
9  
10  
11       **Corresponding author:** Botao Zhou

12       **Corresponding address:** National Climate Center, China Meteorological  
13       Administration, Beijing 100081, China

14       **E-mail:** zhoubt@cma.gov.cn

**Abstract.** Based on the dynamic downscaling by the regional climate model RegCM4 from three CMIP5 global models under the historical and the RCP4.5 simulations, this article evaluated the performance of the RegCM4 downscaling simulations on the air environment carrying capacity (AEC) and weak ventilation days (WVD) in China, which are applied to measure haze pollution potential. Their changes during the middle and the end of the 21st century were also projected. The evaluations show that the RegCM4 downscaling simulations can generally capture the observed features of the AEC and WVD distributions over the period 1986-2005. The projections indicate that the annual AEC tends to decrease and the annual WVD tends to increase almost over the whole country except central China, concurrent with greater change by the late of the 21st century than by the middle of the 21st century. It suggests that annual haze pollution potential would be enlarged under the RCP4.5 scenario as compared to the present. For seasonal change in the four main economic zones of China, it is projected consistently that there would be a higher probability of haze pollution risk over the Beijing-Tianjin-Hebei (BTH) region and the Yangtze River Delta (YRD) region in winter and over the Pearl River Delta (PRD) zone in spring and summer in the context of the warming scenario. Over Northeast China (NEC), future climate change might reduce the AEC or increase the WVD throughout the whole year, which favors the occurrence of haze pollution and thus the haze pollution risk would be aggravated. Relative contribution of different components related to the AEC change further indicates that changes of the boundary layer depth and the wind speed play the leading roles in the AEC change over the BTH and NEC regions. In addition to those

37 two factors, the precipitation change also exerts ~~dominant~~important impacts on the  
38 ~~ACE~~AEC change over the YRD and PRD zones.

39 **Keywords** air environment carrying capacity, ventilation day, haze pollution potential,  
40 regional climate model, evaluation and projection

41



## 1 Introduction

Haze, as a phenomenon of severe air pollution, exerts remarkably adverse impacts on society and human health, thereby highly concerned by the public and policy makers. Particularly in recent years, heavy haze events hit China frequently (Wang et al., 2014; Zhang et al., 2014) and caused serious damages in many aspects. For instance, they not only increased traffic accidents and delayed traffic (Wu et al., 2005; 2008), but also aggravated ill health problems including respiratory disease, heart disease, cancer and premature death (Wang and Mauzerall, 2006; Xu et al., 2013). Thus, more and more attentions have been paid to the haze pollution in China.

The increasing trend of the haze days in China during recent decades (Ding and Liu, 2014; Song et al., 2014) is documented to be largely attributed to human activities. Due to rapid economic development and urbanization, the pollutants emitted into the atmosphere have been increased, consequently resulting in an intensification of haze pollution in China (Liu and Diamond, 2005; He et al., 2013; Wang et al., 2013b; 2016). Climate change also plays an important role (Jacob and Winner, 2009; Wang et al., 2016). Some studies have indicated that the reduction of surface wind speed, surface relative humidity and precipitation in recent decades (Gao, 2008; Guo et al., 2011; Jiang et al., 2013; Song et al., 2014; Ding and Liu, 2014) provide unfavourable conditions for the sedimentation and diffusion of air pollutants, and thus increase the occurrence of haze pollution in China. Besides, the Arctic sea ice declining under global warming contributes positively to the increase of haze days in eastern China (Wang et al., 2015; Wang and Chen, 2016). Other influential climate

factors for the increase of haze pollution in China, such as the weakening of the East Asian winter monsoon (Li et al. 2015; Yin et al., 2015) and the northward shifting of the East Asian jet (Chen and Wang, 2015), are also highlighted. In summary, the combined effects of increased pollutants and climate change are responsible for the haze pollution in China.

IPCC AR5 reported that continued emissions of greenhouse gases will cause further changes in all components of the climate system (IPCC, 2013). From the point of view of the CMIP5 projected change in climate conditions, there are both positive and negative contributors for the haze pollution in China. For example, the projected increase in precipitation (Xu and Xu, 2012; Tian et al., 2015; Wu et al., 2015b) is expected to reduce haze pollution, whereas the decrease of the Arctic sea ice extent (IPCC, 2013) and the weakening of the East Asian winter monsoon (Wang et al., 2013a) are inclined to increase haze pollution. So, how the haze pollution in China will change under the future warming scenario is still an open issue.

Air environment carrying capacity (AEC), which is a combined metric to measure atmospheric capacity in transporting and diluting pollutants into the atmosphere, provides a direct way to investigate the change of the haze pollution potential. When the AEC is low (high), it is unfavourable (favourable) for the diffusion and cleaning of the pollutants, and thus the haze pollution is (not) prone to occur. So far, the AEC has been applied in the operation of China Meteorological Administration (CMA) to forecast haze pollution potential (Kang et al., 2016). On the other hand, CMIP5 global climate models (GCMs) show some limitations in

simulating regional climate due to their relatively coarse resolutions (Giorgi et al., 2009). Regional climate models (RCMs) with higher resolutions are demonstrated to outperform global models on the regional scale (Lee and Hong 2014; Wu et al. 2015a; Gao et al. 2012, 2016b). Thus, this study is aimed to project changes of the haze pollution potential in China from the AEC perspective, based on the downscaling simulations of the regional climate model RegCM4 under the RCP4.5 scenario.

## **2 Model, data and method**

### **2.1 Data, regional climate model and simulations**

The regional climate model RegCM4 used in this study is developed by the ICTP (Giorgi et al., 2012) and applied widely around the world. The model has the horizontal resolution of 25 km and 18 vertical sigma layers with the top at 50 hPa. Based on the study of Gao et al. (2016a, b), we selected a suite of physical parameterization schemes suitable for the simulation of China climate, including the Emanuel convection scheme (Emanuel, 1991), the radiation package of the CCM3 model for atmospheric radiative transfer (Kiehl et al., 1998), the non-local formulation of Holtslag (Holtslag et al., 1990) for planetary boundary layer, the SUBEX parameterization for large-scale precipitation (Pal et al., 2000), and the CLM3.5 for land surface process (Oleson et al., 2008). The land cover data were updated based on the vegetation regionalization maps of China (Han et al., 2015).

The domain for the downscaling simulations is the region recommended by CORDEX-East Asia phase II (Giorgi et al., 2009), covering China continent and

adjacent regions. The RegCM4 simulations, called EC, HAD, and MPI for short, were driven at 6-hourly intervals by the historical (1979-2005) and RCP4.5 (2006-2099) simulations from three CMIP5 global models i.e., EC-EARTH, HadGEM2-ES, and MPI-ESM-MR, respectively. In CMIP5, ~20 GCMs provide the six-hourly outputs of wind speed, temperature, and humidity for dynamical downscaling. However, to drive RCM modeling, the ratio of the resolution between GCMs and RCMs should not exceed 6-8. So, only those GCMs with the resolution of 1~2 degree can be used to drive RegCM4 simulations. Due to the availability of CMIP5 GCMs and considering large volume of outputs for ~120-yr RegCM4 simulations, we just used these three GCMs for this study. The average of the three simulations with equal weight is taken as the ensemble mean. The historical simulation denotes the past climate, and the RCP4.5 represents the medium-low radiative forcing scenario with the radiative forcing peaking at  $4.5 \text{ Wm}^{-2}$  by 2100 (Taylor et al., 2012). Readers can visit <http://cmip-pcmdi.llnl.gov/cmip5> for the information about the three CMIP5 models and the forcing.

To validate the performance of the RegCM4 downscaling simulations, the ERA-Interim reanalysis dataset (Uppala et al., 2008) with the horizontal resolution of ~~1.50.75~~  $1.50.75^\circ \times 1.50.75^\circ$  was employed as observations, including 6-hourly boundary layer height, precipitation, geopotential height and wind speed.

## 2.2 Analysis method

The AEC considers the processes of wet deposition and ventilation and is expressed in the form:

$$AEC = C_s \cdot (W_r \cdot R \cdot \sqrt{S} + \frac{\sqrt{\pi}}{2} \cdot U_{BL} \cdot H) \quad (1)$$

where  $C_s$  is the standard concentration of air pollutant (here, the value is  $75 \mu g m^{-3}$ , standard concentration for  $PM_{2.5}$  in China),  $W_r$  is washout constant ( $6 \times 10^5$ ),  $R$  is precipitation,  $S$  is unit area and defined as  $2500 km^2$ ,  $U_{BL}$  is mean wind speed averaged within the boundary layer,  $H$  is boundary layer height (Xu and Zhu, 1989). High (Low) AEC is disadvantageous (advantageous) for the occurrence of haze pollution, indicating low (high) haze pollution potential. It should be pointed out that the AEC measures atmospheric carrying capacity in transporting and diluting pollutants. It does not reflect real emission characteristics. The  $C_s$  is the standard concentration of air pollutant not the real concentration of the pollutant emitted into the air. For different pollutants, different value can be fixed for  $C_s$ . Because what we concerned in this study is the haze pollution potential, its value is set as the standard concentration for  $PM_{2.5}$  in China.

The term  $U_{BL} \cdot H$  is named ventilation coefficient (Krishnan and Kunhikrishnan, 2004). Large ventilation coefficient means that a deeper boundary layer can dilute pollutants and strong winds can remove local pollutants, unfavourable for the haze occurrence, and vice versa. If each of the 6-hourly ventilation coefficients within one day is less than  $6000 m^2 s^{-1}$ , this day is counted as one weak ventilation day (WVD)

(Leung and Gustafson, 2005). Longer WVD indicates more haze pollution incidents.

The threshold of  $6000 m^2 s^{-1}$  for the ventilation coefficient was widely used not only in the U.S. (Hanson and McKee, 1983; Leung and Gustafson, 2005; Trail et al., 2013), but also in other places such as India (Goyal and Rao, 2007; Manju et al., 2002).

Athens (Kassomenos et al., 1995), and Thailand (Pimonsree, 2008). A sensitivity analysis shows that that there is little change in the relationship between the WVD and the haze days if using different thresholds to calculate WVD.

According to Eq. (1), the AEC change results from changes in precipitation, wind speed, and boundary layer depth, which can be simplified as:

$$\Delta AEC = \alpha \cdot \Delta R + \beta \cdot \Delta(U_{BL} \cdot H) \quad (2)$$

where  $\alpha = C_s \cdot W_r \cdot R$ ,  $\beta = C_s \cdot \frac{\sqrt{\pi}}{2}$ , and  $\Delta$  represents the difference between the future and present-day climate (RCP4.5 minus reference period).

The Eq. (2) could be further decomposed as follows:

$$\Delta AEC = \alpha \cdot \Delta R + \{\beta \cdot \Delta U_{BL} \cdot H_{pd} + \beta \cdot (U_{BL})_{pd} \cdot \Delta H + \beta \cdot \Delta U_{BL} \cdot \Delta H + TR\} \quad (3)$$

The subscript “pd” denotes the present-day climate. The first to third terms in the right-hand side are associated with changes in precipitation, wind speed within the boundary layer, and boundary layer depth, respectively. The fourth term is a nonlinear term including the contribution of changes in both wind speed and boundary layer depth. Since we use 6-hourly data for the AEC calculation while monthly mean data for the diagnosis of the change, the last term TR (transient term, deviation from monthly mean) cannot be ignored, which is obtained as a residual.

The pattern-amplitude projection (PAP) method (Park et al., 2012) is applied to quantify the relative contributions of individual processes  $P_i$  to the AEC change over certain region.

$$P_i = \frac{\langle \Delta AEC_i \cdot \Delta AEC \rangle}{\langle \Delta AEC \cdot \Delta AEC \rangle} \quad (4)$$

in which  $\langle \rangle$  represents area mean,  $\Delta AEC_i$  represents components in the

right-hand side of Eq. (3).

As stated above, a low (high) AEC are favourable (unfavourable) for the occurrence of the haze pollution. Longer (Shorter) WVD corresponds to more (less) haze pollution incidents. To verify this conclusion, we calculated the quantized relationship of the haze days with the AEC and the WVD during the period 1980-2016 in the observation. The data of the haze days, which are based on daily visibility and relative humidity records from ~2400 observation stations in China, are available from the CMA. The correlation analysis does show significantly negative correlations between the haze days and the AEC, and significantly positive correlations between the haze days and the WVD over eastern China where the haze mainly occurs.

### **3 Performance of the downscaling simulations**

The performance of the RegCM4 downscaling simulations on the AEC spatial pattern is firstly evaluated through the comparison with the observation. As shown in Fig. 1a, the observed AEC is in general large in western China, with the maxima located over Tibet. Low AEC is found mainly over central and eastern China, northwestern Xinjiang, and parts of Northeast China. The simulated AEC distributions from the ensemble (Fig. 1b) and its members (Fig. 1c-e) show general resemblance to the observation. The spatial correlation coefficients between the simulation and the observation are all higher than 0.75 (Table 1). On the national average, the root mean square error (RMES) is small for the ensemble mean and each



member, which varies between 0.47 and ~~0.54~~[0.53](#) (Table 1). Nevertheless, there are also some deficits in the simulations. For example, the AEC is underestimated over the southern Xinjiang and overestimated over parts of North China. [Our analysis indicates that the simulation bias in boundary layer depth is the major factor for the simulated AEC bias over most parts of China \(figure not shown\).](#)

We further present the observed and simulated distribution of the seasonal AEC in China during 1986-2005. For the observation, the winter AEC is the lowest among the four seasons in a broad region of China (Fig. 2a). In spring, the AEC increases significantly and the regions with high AEC expand obviously. The central eastern China is dominated by the low capacity (Fig. 2c). Compared with the case in spring, the summer AEC increases over central China while decreases slightly over Tibet and Northeast China (Fig. 2e). The AEC distribution in autumn is similar to that in winter but with larger capacity over the regions except Tibet (Fig. 2g). The seasonal variation of the AEC in the ensemble simulation agrees with that in the observation although there are some discrepancies (Fig. 2b, 2d, 2f and 2h). The spatial correlation coefficient between the simulation and the observation ranges from ~~0.64~~[0.60](#) to 0.79 and the RMES is in the range of 0.47 to ~~0.76~~[0.75](#) for the national average in four seasons (Table 2).

The WVD distribution during 1986-2005 in the observation and the ensemble simulation is displayed in Fig. 3a and Fig.3b, respectively. It is noticed that the simulated pattern and the observed pattern are approximate to each other. Namely, the number of weak ventilation days per year is relatively small over Tibet while

relatively large over central and eastern China, Northeast China, southern North China and Xinjiang. The spatial correlation between them is [0.740.75](#). However, we also note that the WVD is overestimated by the ensemble simulation.

The wet deposition is observed to be large over southern China and the south edge of the Tibetan Plateau while small over northwestern China (Fig. 3c). According to Eq. (1), the wet deposition pattern exactly corresponds to the distribution of precipitation. The observed features can also be captured by the ensemble simulation (Fig. 3d). The spatial correlation coefficient between the simulation and the observation is up to [0.840.85](#).

In brief, the downscaling simulations of the RegCM4 can reasonably reproduce the observed characteristics of the distribution of the AEC, WVC and wet deposition in China. It provides justification to use them for the future projection.

#### **4 Projected changes**

Fig. 4 exhibits the ensemble projected changes in AEC, WVC and wet deposition during the middle of the 21st century (2046-2065) and the end of the 21st century (2080-2099) relative to the reference period 1986-2005. The periods 2046-2065 and 2080-2099 are commonly used to represent near-term and long-term in the CMIP5 projection, respectively (IPCC, 2013). A general decrease in AEC and an overall increase in WVC are projected over almost the whole country except central China in the context of the RCP4.5 scenario. The change in magnitude is larger by the end of the 21st century than by the middle of the 21st century. The maximum decrease in

AEC appears at the edge of the Qinghai-Tibet Plateau and the Loess Plateau, with the percentage change being 4% for the middle of the 21st century and 5% for the end of the 21st century. The relatively large decreases are located in Southwest China, northern North China, Northeast China and Inner Mongolia (Fig. 4a and Fig.4b). The increase in WVD is projected to be particularly pronounced in western and northern China (Fig. 4c and Fig. 4d). The three ensemble samples agree well on the sign of the changes, indicative of a good consistency in the projection. In contrast, there would be an increasing tendency for the AEC and a decreasing tendency for the WVD over central China where the climatological capacity is low in the reference period 1986-2005. However, the sign of the projected change is inconsistent among the three ensemble samples. Compared with the ensemble projection, the EC and HAD show relatively large discrepancy for the sign of the projected change in AEC and WVD, respectively (Figures not shown).

For the change in wet deposition, a general increase is projected across China, also with greater change in 2080-2099 than in 2046-2065 (Fig. 4e and Fig. 4f). In addition, we can find inconsistent signs of the projected change over southern China during 2046-2065 (Fig. 4e) and over some parts of Northeast China during 2080-2099 (Fig. 4f). The inconsistent during 2046-2065 (2080-2099) is mainly due to the difference of the HAD (MPI) projection from the other two ensemble members (Figures not shown).

Following, we turn to examine the seasonal and annual changes of the AEC and WVD over the four main economic zones of China [\(Fig. 1f\)](#) which suffer severely

from the haze pollution at present, i.e., Beijing-Tianjin-Hebei region (BTH), Northeast China (NEC), Yangtze River Delta economic zone (YRD), and Pearl River Delta economic zone (PRD) in more detail.

#### 1) Beijing-Tianjin-Hebei region

As shown in Fig. 5a, the ensemble projection indicates a decrease of the AEC in all four seasons during the middle of the 21st century. The percentage change relative to 1986-2005 is the lowest in spring and the largest in winter. The changes in summer and autumn are between -2% and -3%. The three ensemble members agree on the sign of the changes in all seasons except spring but with different spread. For the summer season, the spread is the smallest. While in other seasons, it is close to or larger than the ensemble projected change. During the end of the 21st century, the decrease of the AEC is further enhanced, with the largest enhancement occurring in winter. Moreover, the spread in general becomes much larger. For annual change, both the ensemble and its members project that the AEC would reduce during the middle and the end of the 21st century with the larger amplitude in the latter period.

As for the WVD (Fig. 5b), an increasing tendency is projected by the ensemble for annual and seasonal mean during the middle of the 21st century. The change is the smallest in summer and the largest in winter. The ensemble members show good agreement on the positive change in winter, autumn, and annual mean. During the late of the 21st century, the increase in WVD is further enlarged in winter and autumn while it is reduced in spring and summer. There is no appreciable change for annual mean as compared to that in the middle of the 21st century. Only for the winter season

and annual mean, all the individual simulations consistently show the same projection as the ensemble.

## 2) Northeast China

The annual and seasonal AEC is projected by the ensemble to decrease during the middle of the 21st century, and the percentage changes are comparable among four seasons and annual mean (Fig. 6a). The ensemble members also project negative tendency consistently except in spring. Compared with the middle of the 21st century, the case for the end of the 21st century is similar but with larger decrease. Besides, all the three ensemble members show good consistence for the projection.

The WVD is projected by the ensemble and its members to increase during the middle and the end of the 21st century for annual mean and all four seasons (Fig. 6b). Similarly, the projected change is larger during the end of the 21st century than during the middle of the 21st century, with the largest increase appearing in spring.

## 3) Yangtze River Delta economic zone

The ensemble projection indicates that the AEC would decrease for annual mean and all the seasons except autumn (Fig. 7a). The percentage change is the smallest in spring (with the decrease of less than 1%) and the greatest in winter (with the decrease of more than 3%). The counterparts for summer and autumn are about -2% and 1%, respectively. However, large spread exists among the projections of the three ensemble members. Only for winter and annual mean, they project the same sign of the change. At the end of the 21st century in the ensemble projection, the decrease in AEC is enhanced to 6% in winter. Consistent change is projected by the ensemble

members. In contrast, the decrease in summer and the increase in autumn are weakened as compared to the middle of the 21st century. A slight increase of the AEC is found in spring. For annual mean AEC, the decrease is somewhat larger by the end of the 21st century than by the middle of the 21st century.

The WVD for annual mean, winter and spring is projected by the ensemble to increase, with larger change during the end of the 21st century than during the middle of the 21st century (Fig. 7b). The greatest change occurs in winter. For summer, the ensemble projects that the WVD almost remains unchanged during the middle of the 21st century while increases at the end of the 21st century. For autumn, the ensemble projects that the WVD decreases slightly during the middle of the 21st century while increases slightly by the end of the 21st century. The ensemble members show good consistency of the projections for winter and annual mean during both periods.

#### 4) Pearl River Delta economic zone

As projected by the ensemble (Fig. 8a), the annual, spring and summer AEC would decrease. Such a decrease is relatively larger during the middle of the 21st century than during the end of the 21st century and the greatest decrease occurs in spring. For winter, the AEC is projected to increase and be comparable during the middle and the end of the 21st century. For autumn, the projected AEC decreases by about 1% over the period 2046-2065 and increase by about 0.5% over the period 2080-2099. However, the projections from the three members are not consistent for all four seasons.

The ensemble projects an increase in WVD for annual mean and four seasons, with the greatest increase in summer during the middle of the 21st century (Fig. 8b). The individual members consistently show the positive change for spring, summer, and annual mean. Compared with the middle of the 21st century, the increase of the WVD is reduced in summer while enhanced for annual mean and the remaining seasons during the late of the 21st century. The autumn is the season with the maximum change. The individual members show the same projections as the ensemble on the sign of change still for spring, summer, and annual mean.

The consistence of the three ensemble members on the direction of the projected change which can be used to visualize the uncertainty in the projection is further summarized in Table 3. In general, although there are some uncertainties on the regional changes, the three members consistently project a decrease of the AEC or an increase of WVD for annual mean over the four economic zones, especially over the Beijing-Tianjin-Hebei region and Northeast China. It signifies that future climate change will contribute positively to the haze pollution in these regions. For seasonal change, decrease in AEC or increase in WVD, is projected consistently to appear in all four seasons over Northeast China. It suggests that there would be an increase of haze pollution potential throughout the whole year. Besides, the consistent projections indicate a higher potential risk of haze pollution over the Beijing-Tianjin-Hebei region and the Yangtze River Delta region in winter and over the Pearl River Delta zone in spring and summer.



The temporal evolution of the annual and seasonal AEC and WVD over the four main economic zones are also plotted (Figs. 5-8 c-g), and the corresponding trend values projected by the ensemble for the period of 2016-2099 are summarized in Table 4. Theil-Sen trend analysis (Theil, 1950; Sen, 1968) was used to estimate the trends and the non-parametric Mann-Kendall test (Mann, 1945; Kendall, 1975) was used for significant test. Generally, the secular variations of the AEC and the WVD show some diversity across different seasons over the regions except NEC where a decrease in AEC and an increase in VWD is projected uniformly. Nevertheless, for the trends significant above the 95% level, it is interesting to notice that the decrease in AEC is mostly accompanied with the increase in WVD, for instance for winter over TBH, for annual mean and all the seasons over NEC, for annual mean, winter and summer over YRD, and for annual mean and autumn over PRD.

## **5 Contributions of different factors to the change of AEC**

Based on Eqs. (2) and (3), we further investigate the contribution of different factors to the projected change in AEC. For brevity, we only show the results for the period 2046-2065 in the following, because the case for the period 2080-2099 is similar.

Figs. 9a and 9b exhibit relative contributions to the annual AEC change over the course of 2046-2065 from changes in precipitation and ventilation, respectively. Overall, the ventilation change plays a dominant role in and contributes positively to the change of the AEC over most parts of China, particularly in western and northern

China (Fig. 9b). In contrast, the relative contribution of the precipitation change is in general negative over western and northern China while positive over southern China (Fig. 9a).

According to Eq. (3), the effect of ventilation change can be decomposed into four terms, i.e., wind speed change, boundary layer depth change, nonlinear term, and transient term. Among these contributors for annual ventilation change, the effects of boundary layer depth (Fig.9d) and wind speed (Fig.9c) are relatively large and the former is greater than the latter over most parts of eastern China. The transient term also exert effects for instance over some parts of western and southern China (Fig.9f), while the effects of the nonlinear term are tiny across China (Fig. 9e).

Fig. 10 further presents relative contributions of aforementioned factors to annual and seasonal AEC change over the four economic zones as projected by the ensemble and its members. As shown in Figs. 10a and 10b, changes in wind speed and boundary layer depth have the greatest contributions to the AEC change over the THB and NEC regions for annual mean and all the seasons except summer. The contribution from the precipitation is in general relatively small. Besides, the effects of the transient term are larger than that of the precipitation, and the effects of the nonlinear term can be negligible. These results indicate that changes in wind speed and boundary layer depth are the leading contributors responsible for the AEC change over the two regions. In contrast, over the YRD (Fig.10c) and PRD (Fig.10d) zones, change in precipitation also plays ~~an important~~ dominant role. The contribution from

the precipitation change is comparable to and even larger than that from changes in wind speed and boundary layer depth for all the seasons except winter.

## **6 Conclusion**

In this study, we conducted downscaling simulations by use of the RegCM4 driven by three CMIP5 models' results under the historical simulation and the RCP4.5 scenario. On this basis, we evaluated the fidelity of the RegCM4 simulations on the AEC and WVD which are indicators for haze pollution potential, and then projected their change during the middle and the end of this century for China and four main economic zones. The major findings are summarized below:

1) The evaluation indicates that the RegCM4 downscaling simulations in general show good performance in modeling the climatological distribution of the annual and seasonal AEC, despite some discrepancies in certain regions. The spatial correlations between the simulation and the observation for annual mean and four seasons are higher above 0.6. The simulations also well capture the observed WVD pattern with relatively small WVD over Tibet and relatively large WVD over central and eastern China, Northeast China, southern North China and Xinjiang, although the WVD is overestimated systematically.

2) The annual AEC and WVD are respectively projected by the ensemble to decrease and increase almost in the entire region except central China, accompanied with larger amplitude by the end of the 21st century than by the middle of the 21st century. The decreases in AEC are relatively large over Tibet, Southwest China,

northern North China, Northeast China and Inner Mongolia. The increase in WVD is particularly pronounced in northern China. The individual members present consistent projections of changes as the ensemble. In contrast, the ensemble projects an increase in AEC and a decrease in WVD over central China. However, the sign of the projected change is inconsistent among the ensemble samples.

3) The consistency analysis suggests that there would be a high probability of the increase in air pollution risk over the BTH and YRD regions in winter and over the PRD zone in spring and summer in a warmer world. Over NEC, climate change might reduce the AEC or increase the WVD throughout the whole year, favorable for the occurrence of haze pollution and also indicative of an aggravation of haze pollution risk. Furthermore, the contribution analysis indicates that changes in boundary layer depth and wind speed play the leading roles in the AEC change over the BTH and NEC regions. In addition to the aforementioned two factors, the precipitation change is also [a dominantan important](#) factor influencing the ACE change over the YRD and PRD zones.

In this study, we mainly showed the downscaled results driven by three global models. Note that the planetary boundary layer depth is not a standard CMIP5 output variable, and the coarse vertical resolution of the global models prevents us from estimating the planetary boundary layer depth. ~~Moreover, the CMIP5 experiments did not supply high-frequency (six-hourly) outputs for calculating AEC and WVD.~~ These make it hard to estimate whether the consistencies and inconsistencies of the projection is caused by the global models or to some extent affected by the dynamical

downscaling of the regional model. Besides, it should be emphasized again that our study focused on the atmospheric carrying capacity which is associated with the wet deposition and the ventilation. It is just one of the contributors for the haze change. Other factors such as emission, wind direction, relative humidity are also vital for the incident of haze. To get a full picture for future change of the haze, their effects need to be studied by models with chemistry/aerosol module coupled in the future work.

442 **Acknowledgments.** This research was jointly supported by the National Key  
443 Research and Development Program of China (2016YFA0600701), the National  
444 Natural Science Foundation of China (41675069, 41405101), and the Climate Change  
445 Specific Fund of China (CCSF201626, [CCSF201731](#)).

## References

- Chen, H. P. and Wang, H. J.: Haze days in North China and the associated atmospheric circulations based on daily visibility data from 1960 to 2012, *J. Geophys. Res. Atmos.*, 120, 5895–5909, doi:10.1002/2015JD023225, 2015.
- Ding, Y. H., and Liu, Y. J.: Analysis of long-term variations of fog and haze in China in recent 50 years and their relations with atmospheric humidity, *Sci. China Earth Sci.*, 57, 36–46, 2014.
- Emanuel, K. A.: A scheme for representing cumulus convection in large-scale models, *J. Atmos. Sci.*, 48, 2313–2329, 1991.
- Gao, G.: The climatic characteristics and change of haze days over China during 1961–2005, *Acta Geogr. Sin.*, 63, 762–768, 2008.
- Gao, X., Shi, Y., Zhang, D., Wu, J., Giorgi, F., Ji, Z., and Wang, Y.: Uncertainties in monsoon precipitation projections over China: results from two high-resolution RCM simulations, *Clim. Res.*, 52, 213–226, 2012.
- Gao, X., Shi, Y., and Giorgi, F.: Comparison of convective parameterizations in RegCM4 experiments over China with CLM as the land surface model, *Atmos. Ocean. Sci. Lett.*, 9, 246–254, 2016a.
- Gao, X., Shi, Y., Han, Z., Wang, M., Wu, J., Zhang, D., Xu, Y., and Giorgi, F.: Performance of RegCM4 over major river basins in China, *Adv. Atmos. Sci.*, doi:10.1007/s00376-016-6179-7, 2016b.
- Giorgi, F., Jones, C., and Asrar, G.: Addressing climate information needs at the regional level: the CORDEX framework, *WMO Bull.*, 58, 175–183, 2009.



Giorgi, F., Coppola, E., Solmon, F., Mariotti, L., Sylla, M., Bi, X., Elguindi, N., Diro,  
 G., Nair, V., Giuliani, G., Turuncoglu, U., Cozzini, S., Güttler, I., O'Brien, T.,  
 Tawfik, A., Shalaby, A., Zakey, A., Steiner, A., Stordal, F., Sloan, L., and  
 Brankovic, C.: RegCM4: model description and preliminary tests over multiple  
 CORDEX domains, *Clim. Res.*, 52, 7–29, 2012.

Goyal, S., and Rao, C. C.: Air assimilative capacity-based environment friendly siting  
 of new industries - A case study of Kochi region, India, *J. Environ. Manage.*, 84,  
 473-483, 2007.

Guo, H., Xu, M., and Hu, Q.: Changes in near-surface wind speed in China: 1969–  
 2005, *Int. J. Climatol.*, 31, 349–358, 2011.

Han, Z., Gao, X., Shi, Y., Wu, J., Wang, M., and Giorgi, F.: Development of Chinese  
 high resolution land cover for the RegCM4/CLM and its impact on regional  
 climate simulation (in Chinese), *Journal of Glaciology and Geocryology*, 37,  
 857–866, 2015.

He, H., Wang, X. M., Wang, Y. S., Wang, Z. F., Liu, J. G., Chen, Y. F., 2013:  
 Formation mechanism and control strategies of haze in China (in Chinese), *Bull.  
 Chinese Acad. Sci.*, 28(3), 344–352.

Holtzlag, A. A. M., De Bruijn, E. I. F., and Pan, H. L.: A high resolution air mass  
 transformation model for short-range weather forecasting, *Mon. Wea. Rev.*, 118,  
 1561–1575, 1990.

IPCC: Climate Change 2013: The Physical Science Basis. Contribution of Working  
 Group I to the Fifth Assessment Report of the Intergovernmental Panel on Climate

490 Change, Cambridge University Press, Cambridge, United Kingdom and New  
 491 York, NY, USA, 1535pp, 2013.

492 Kassomenos, P., Kotroni, V., and Kallos, G.: Analysis of climatological and air  
 493 quality observations from greater Athens area, Atmos. Environ., 29, 3671-3688,  
 494 1995.

495 Manju, N., Balakrishnan, R., and Mani, N.: Assimilative capacity and pollutant  
 496 dispersion studies for the industrial zone of Manali, Atmos. Environ., 36,  
 497 3461-3471, 2002.

498 Jacob, D. J., and Winner, D. A.: Effect of climate change on air quality, Atmos.  
 499 Environ., 43, 51-63, 2009.

500 Jiang, Y., Luo, Y., and Zhao, Z. C.: Maximum wind speed changes over China, Acta  
 501 Meteorol. Sin., 27, 63–74, 2013.

502 Kang, Z., Gui, H., Hua, C., Zhang, B., Zhang, H., Lv, M., and Wang, J.: National  
 503 Environmental Meteorological Services in China, Adv. Meteorol., 2016, doi:  
 504 10.1155/2016/1985207, 2016.

505 Kendall, M. G.: Rank Correlation Methods. Griffin, London, 1975.

506 Kiehl, J., Hack, J., Bonan, G., Boville, B., Williamson, D., and Rasch, P.: The  
 507 National Center for Atmospheric Research Community Climate Model: CCM3, J.  
 508 Clim., 11, 1131–1149, 1998.

509 Krishnan, P., and Kunhikrishnan, P.: Temporal variations of ventilation coefficient at  
 510 a tropical Indian station using UHF wind profiler, Curr. Sci, 86, 447–451, 2004.

511 Lee, J., and Hong, S.: Potential for added value to downscaled climate extremes over  
512 Korea by increased resolution of a regional climate model, *Theor. Appl.*  
513 *Climatol.*, 117, 667–677, 2014.

514 Leung, L. R., and Gustafson, W. I.: Potential regional climate change and  
515 implications to US air quality, *Geophys. Res. Lett.*, 32, L16711, 2005.

516 Li, Q., Zhang, R. H., and Wang, Y.: Interannual variation of the winter-time fog–haze  
517 days across central and eastern China and its relation with East Asian winter  
518 monsoon, *Int. J. Climatol.*, 36, 346–354, doi:10.1002/joc.4350, 2015.

519 Liu, J., and Diamond, J.: China’s environment in a globalizing world, *Nature*, 435,  
520 1179–1186, 2005.

521 Mann, H. B.: Nonparametric tests against trend, *Econometrica*, 13, 245–259, 1945.

522 Oleson, K., Niu, G. Y., Yang, Z. L., Lawrence, D., Thornton, P., Lawrence, P.,  
523 Stöckli, R., Dickinson, R., Bonan, G., and Levis, S.: Improvements to the  
524 Community Land Model and their impact on the hydrological cycle, *J. Geophys.*  
525 *Res.*, 113, G01021, 2008.

526 Pal, J. S., Small, E. E., and Eltahir, E. A. B.: Simulation of regional-scale water and  
527 energy budgets: Representation of subgrid cloud and precipitation processes  
528 within RegCM, *J. Geophys. Res.*, 105, 29579–29594, 2000.

529 Park, T. W., Deng, Y., and Cai, M.: Feedback attribution of the El Niño–Southern  
530 Oscillation–related atmospheric and surface temperature anomalies, *Journal of*  
531 *Geophysical Research: Atmospheres*, 117, D23101, doi:10.1029/2012jd018468,  
532 2012.

533 [Pimonsree, S.: PM10 dispersion during air pollution episode in Saraburi, Thailand,](#)

534 [Asia-Pacific Journal of Science and Technology, 13, 1185-1190, 2008.](#)

535 Sen, P. K.: Estimates of the regression coefficient based on Kendall's tau, Journal of  
536 the American Statistical Association, 63, 1379-1389, 1968.

537 Song, L. C., Gao, R., Li, Y., and Wang, G. F.: Analysis of China's haze days in the  
538 winter half-year and the climatic background during 1961–2012, Adv. Clim.  
539 Change Res., 5, 1–6, 2014.

540 Taylor, K. E., Stouffer, B. J., and Meehl, G. A.: An overview of CMIP5 and the  
541 experiment design, Bull. Am. Meteorol. Soc., 93, 485–498, 2012.

542 Theil, H.: A rank-invariant method of linear and polynomial regression analysis,  
543 Proceedings of the Royal Netherlands Academy of Sciences, 53, I: 386–392, II:  
544 521–525, III: 1397–1412, 1950.

545 Tian, D., Guo, Y., and Dong, W. J.: Future changes and uncertainties in temperature  
546 and precipitation over China based on CMIP5 models. Adv. Atmos. Sci., 32,  
547 487–496, doi:10.1007/s00376-014-4102-7, 2015.

548 [Trail, M., Tsimpidi, A., Liu, P., Tsigaridis, K., Hu, Y., Nenes, A., and Russell, A.:](#)

549 [Downscaling a global climate model to simulate climate change over the US and](#)

550 [the implication on regional and urban air quality, Geoscientific Model](#)

551 [Development, 6, 1429, 2013.](#)

552 Uppala, S., Dee, D., Kobayashi, S., Berrisford, P., and Simmons, A.: Towards a climate  
553 data assimilation system: Status update of ERA-Interim, ECMWF newsletter, 115,  
554 12–18, 2008.

555 Wang, H. J. and Chen, H. P.: Understanding the recent trend of haze pollution in  
 556 eastern China: roles of climate change, *Atmos. Chem. Phys.*, 16, 4205–4211,  
 557 doi:10.5194/acp-16-4205-2016, 2016.

558 Wang, H. J., Chen, H. P., and Liu, J. P.: Arctic sea ice decline intensified haze  
 559 pollution in eastern China, *Atmos. Ocean. Sci. Lett.*, 8, 1–9, 2015.

560 Wang, H. J., He, S. P., and Liu, J. P.: Present and future relationship between the East  
 561 Asian winter monsoon and ENSO: Results of CMIP5, *J. Geophys. Res. Ocean*,  
 562 118, 1–16, doi:10.1002/jgrc.20332, 2013a.

563 Wang, X. P. and Mauzerall, D. L.: Evaluating impacts of air pollution in China on  
 564 public health: implications for future air pollution and energy policies, *Atmos.*  
 565 *Environ.*, 40, 1706–1721, 2006.

566 Wang, Y. S., Yao, L., Liu, Z. R., Ji, D. S., Wang, L. L., and Zhang, J. K.: Formation of  
 567 haze pollution in Beijing-Tianjin-Hebei region and their control strategies, *Bull.*  
 568 *Chinese Acad. Sci.*, 28, 353–363, 2013b.

569 Wang, Z. F., Li, J., Wang, Z., Yang, W. Y., Tang, X., Ge, B. Z., Yan, P. Z., Zhu, L. L.,  
 570 Chen, X. S., Chen, H. S., Wang, W., Li, J. J., Liu, B., Wang, X. Y., Wang, W.,  
 571 Zhao, Y. L., Lu, N., and Su, D. W.: Modeling study of regional severe hazes  
 572 over Mid-Eastern China in January 2013 and its implications on pollution  
 573 prevention and control, *Sci. China: Earth Sci.*, 57, 3–13,  
 574 doi:10.1007/s11430-013-4793-0, 2014.

575 Wu, D., Tie, X., Li, C. C., Ying, Z. M., Lau, A. K., Huang, J., Deng, X. J., and Bi, X.  
 576 Y.: An extremely low visibility event over the Guangzhou region: A case study,  
 577 Atmos. Environ., 39, 6568–6577, 2005.

578 Wu, D., Liao, G. L., Deng, X. J., Bi, X. Y., Tan, H. B., Li, F., Jiang, C. L., Xia, D.,  
 579 and Fan, S. J.: Transport condition of surface layer under haze weather over the  
 580 Pearl River Delta, J. Appl. Meteorol. Sci., 19, 1–9, 2008.

581 Wu, J., Gao, X., Xu, Y., and Pan, J.: Regional climate change and uncertainty analysis  
 582 based on four regional climate model simulations over China, Atmospheric and  
 583 Oceanic Science Letters, 8, 147-152, 2015a.

584 Wu, J., Zhou, B. T., and Xu, Y.: Response of precipitation and its extremes over  
 585 China to warming: CMIP5 simulation and projection, Chinese J. Geophys., 58,  
 586 3048-3060, doi: 10.6038/cjg20150903, 2015b.

587 Xu, D., and Zhu, R.: A study on the distribution of ventilation and rainout capacity in  
 588 mainland China (in Chinese), China Environ. Sci, 9, 367-374, 1989.

589 Xu, P., Chen, Y. F., and Ye, X. J.: Haze, air pollution, and health in China, Lancet,  
 590 382, 2067, doi:10.1016/S0140-6736(13)62693-8, 2013.

591 Xu, Y., and Xu, C. H., Preliminary assessment of simulations of climate changes over  
 592 China by CMIP5 multi-models, Atmos. Ocean. Sci. Lett., 5, 489–494, 2012.

593 Yin, Z. C., Wang, H. J., and Guo, W. L.: Climatic change features of fog and haze in  
 594 winter over North China and Huang-Huai Area, Sci. China Earth Sci., 58, 1370–  
 595 1376, 2015.

596 Zhang, R. H., Li, Q., and Zhang, R. N.: Meteorological conditions for the persistent  
597 severe fog and haze event over eastern China in January 2013, *Sci. China: Earth*  
598 *Sci.*, 57, 26–35, 2014.

**Captions:**

**Table 1.** Statistic results for the simulation skills in annual mean AEC for the period of 1986-2005.

**Table 2.** Statistic results for the ensemble simulation skills in seasonal AEC for the period of 1986-2005.

**Table 3.** The consistence of the three ensemble members on the direction of the projected change over the four economic zones of China. Consistent projection on the decrease in AEC is marked by  $\surd$  and that on the increase in WVD is marked by  $\star$ .

**Table 4.** Trends of AEC and WVD (%/10a) over the four economic zones of China, based on 9-year running mean time series of the percentage change during 2016-2099. Asterisks indicate the trends are statistically significant above the 95% confidence level.

**Figure 1.** Spatial distribution of annual AEC (unit:  $10^4\text{t/a/km}$ ) during 1986-2005: (a) observation, (b) ensemble, (c) EC, (d) HAD, (e) MPI. [\(f\) Four main economic zones of China, Beijing-Tianjin-Hebei region \(BTH\), Northeast China \(NEC\), Yangtze River Delta economic zone \(YRD\), and Pearl River Delta economic zone \(PRD\).](#)

**Figure 2.** Spatial distribution of seasonal AEC (unit:  $10^4\text{t/a/km}$ ) during 1986-2005: (a-b) winter, (c-d) spring, (e-f) summer, (g-h) autumn. Left panel is for the observation and the right panel is for the ensemble simulation.



**Figure 3.** Spatial distribution of (a-b) the number of weak ventilation days per year and (c-d) wet deposition (unit:  $10^4\text{t/a/km}$ ) during 1986-2005: (a, c) observation, (b, d) ensemble simulation.

**Figure 4.** Ensemble projected percentage changes (relative to 1986-2005) in (a-b) AEC and (c-d) WVD during (a, c) 2046-2065 and (b, d) 2080-2099. Hatched regions indicate all ensemble members agree on the sign of change.

**Figure 5.** Range of projected percentage changes (relative to 1986-2005) in (a) AEC and (b) WVD during 2046-2065 and 2080-2099, and 9a running mean time series of percentage changes in (c) annual, (d) winter (DJF), (e) spring (MAM), (f) summer (JJA), (g) autumn (SON) for the Beijing-Tianjin-Hebei region. In Figure (a-b), the bars represent the ensemble projection and the marks represent the individual projection of the three members; the left (right) bar in each group is for 2046-2065 (2080-2099). In Figure (c-g), the solid (dashed) lines represent changes in AEC (WVD).

**Figure 6.** Same as Figure 5, but for Northeast China.

**Figure 7.** Same as Figure 5, but for Yangtze River Delta economic zone.

**Figure 8.** Same as Figure 5, but for Pearl River Delta economic zone.

**Figure 9.** Relative contributions (unit: %) of individual components to annual AEC change in the middle of the 21st century based on the ensemble results. (a) precipitation, (b) ventilation, (c) wind speed averaged with the boundary layer, (d) boundary layer depth, (e) nonlinear term, (f) transient term.

**Figure 10.** Relative contributions (unit: %) of individual components to annual AEC change in the middle of the 21st century averaged over four main economic zones of China: (a) BTH, (b) NEC, (c) YRD, (d) PRD. The bars represent the ensemble projection and the marks represent the individual projection of the three members. Bars from left to right in each group are in turn for annual, DJF, MAM, JJA, and SON.

**Table 1.** Statistic results for the simulation skills in annual mean AEC for the period of 1986-2005.

Simulations	Pattern correlation coefficient (CC)	Root mean square error (RMES)
EC	0.76	0.47
HAD	0.79	<del>0.54</del> 0.53
MPI	<del>0.75</del> 0.76	<del>0.48</del> 0.47
Ensemble	0.77	<del>0.49</del> 0.48

**Table 2.** Statistic results for the ensemble simulation skills in seasonal AEC for the period of 1986-2005.

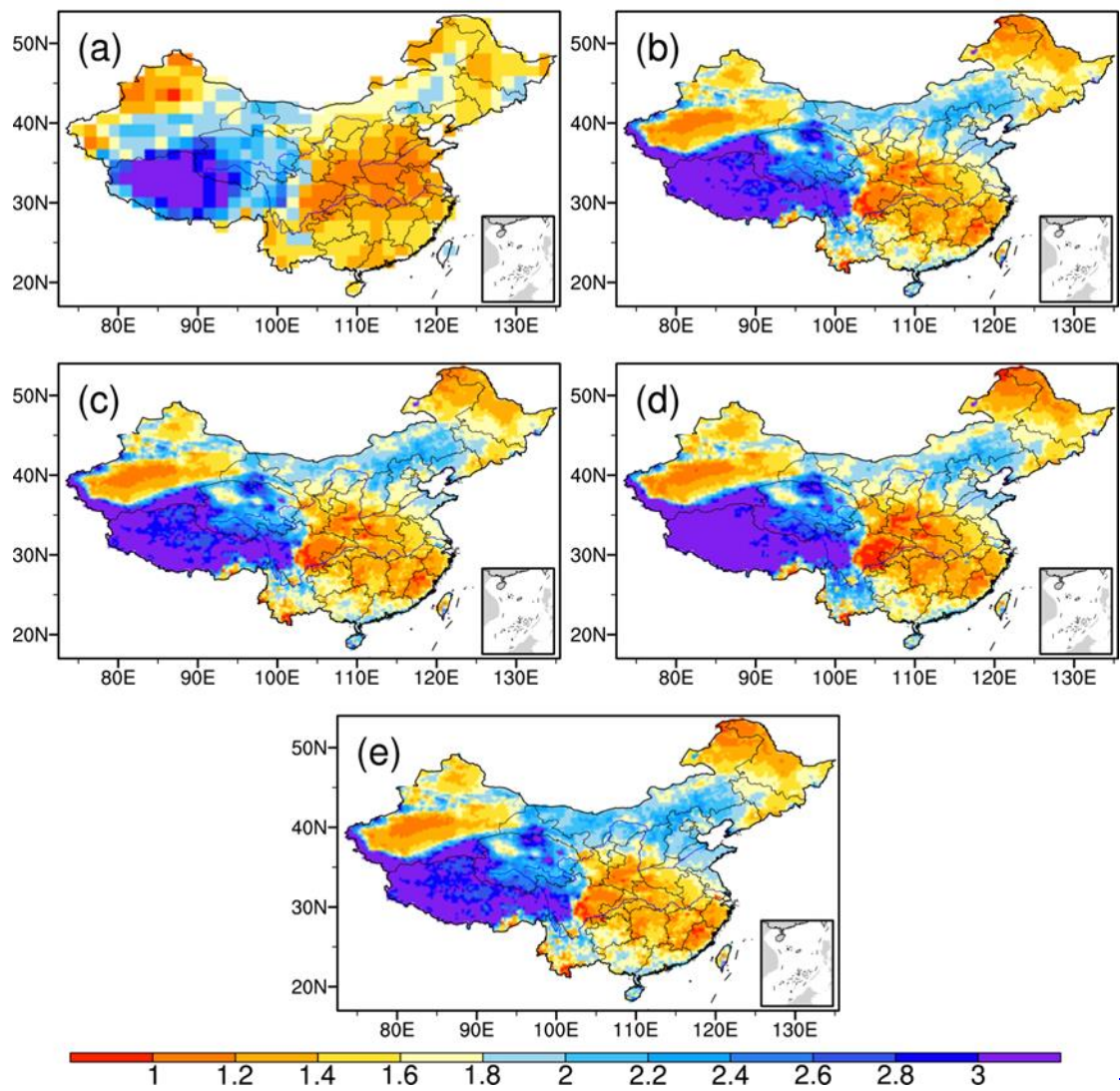
Season	Pattern correlation coefficient (CC)	Root mean square error (RMES)
Winter	0.79	<del>0.76</del> 0.75
Spring	0.75	<del>0.68</del> 0.67
Summer	<del>0.64</del> 0.60	<del>0.56</del> 0.57
Autumn	0.78	0.47

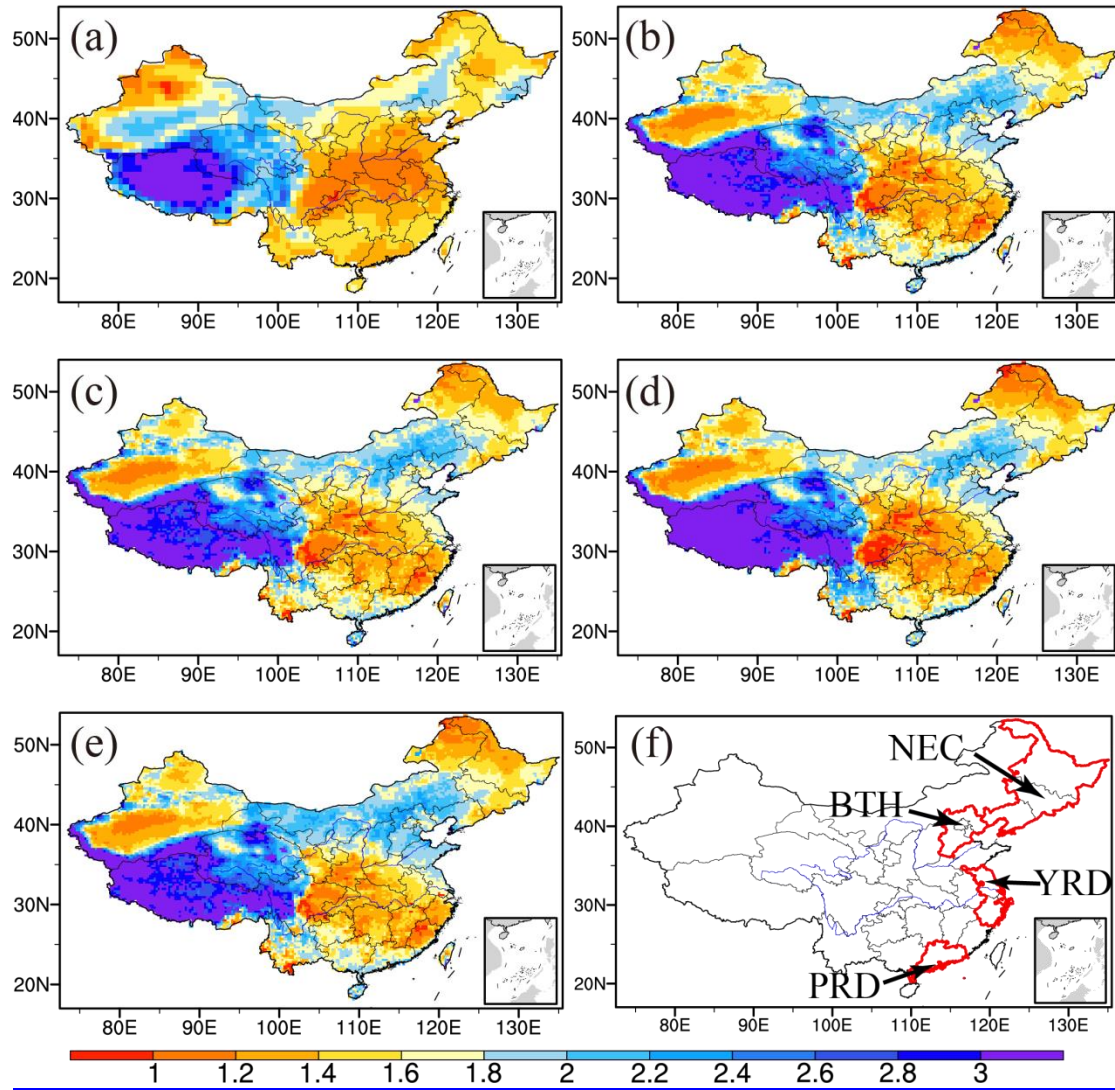
**Table 3.** The consistence of the three ensemble members on the direction of the projected change over the four economic zones of China. Consistent projection on the decrease in AEC is marked by ✓ and that on the increase in WVD is marked by ☆.

Economic zone	Period	ANN	DJF	MAM	JJA	SON
BTH	2046-2065	✓ ☆	✓ ☆		✓	✓ ☆
	2080-2099	✓ ☆	☆			
NEC	2046-2065	✓ ☆	✓ ☆	☆	✓ ☆	✓ ☆
	2080-2099	✓ ☆	✓ ☆	✓ ☆	✓ ☆	✓ ☆
YRD	2046-2065	✓ ☆	✓ ☆			
	2080-2099	☆	✓ ☆			
PRD	2046-2065	☆		☆	☆	
	2080-2099	☆		☆	☆	

**Table 4.** Trends of AEC and WVD (%/10a) over the four economic zones of China, based on 9-year running mean time series of the percentage change during 2016-2099. Asterisks indicate the trends are statistically significant above the 95% confidence level.

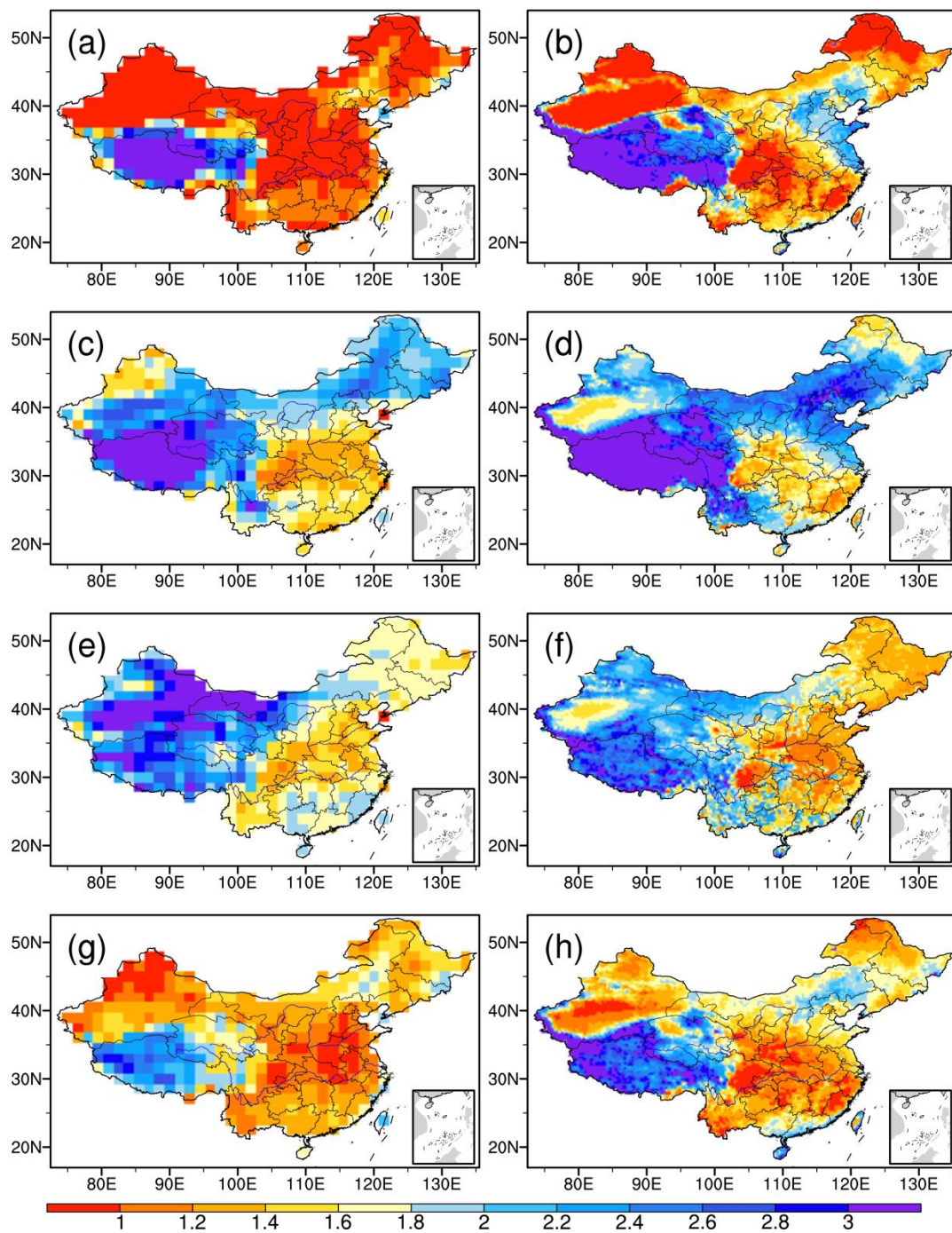
Economic zone	Variable	ANN	DJF	MAM	JJA	SON
BTH	AEC	-0.41*	-0.96*	0.02	-0.19*	-0.80*
	WVD	0.33	2.30*	-1.53*	-0.51*	0.55
NEC	AEC	-0.46*	-0.76*	-0.26*	-0.41*	-0.61*
	WVD	1.49*	2.60*	1.30*	0.73*	0.97*
YRD	AEC	-0.27*	-1.17*	0.32*	-0.45*	-0.02
	WVD	0.51*	0.88*	-0.26	0.71*	-0.15
PRD	AEC	-0.14*	-0.03	-0.22*	-0.12	-0.29*
	WVD	1.17*	-0.01	-0.30	2.17*	1.50*





**Figure 1.** Spatial distribution of annual AEC (unit:  $10^4$  t/a/km) during 1986-2005: (a) observation, (b) ensemble, (c) EC, (d) HAD, (e) MPI. (f) Four main economic zones of China, Beijing-Tianjin-Hebei region (BTH), Northeast China (NEC), Yangtze River Delta economic zone (YRD), and Pearl River Delta economic zone (PRD).





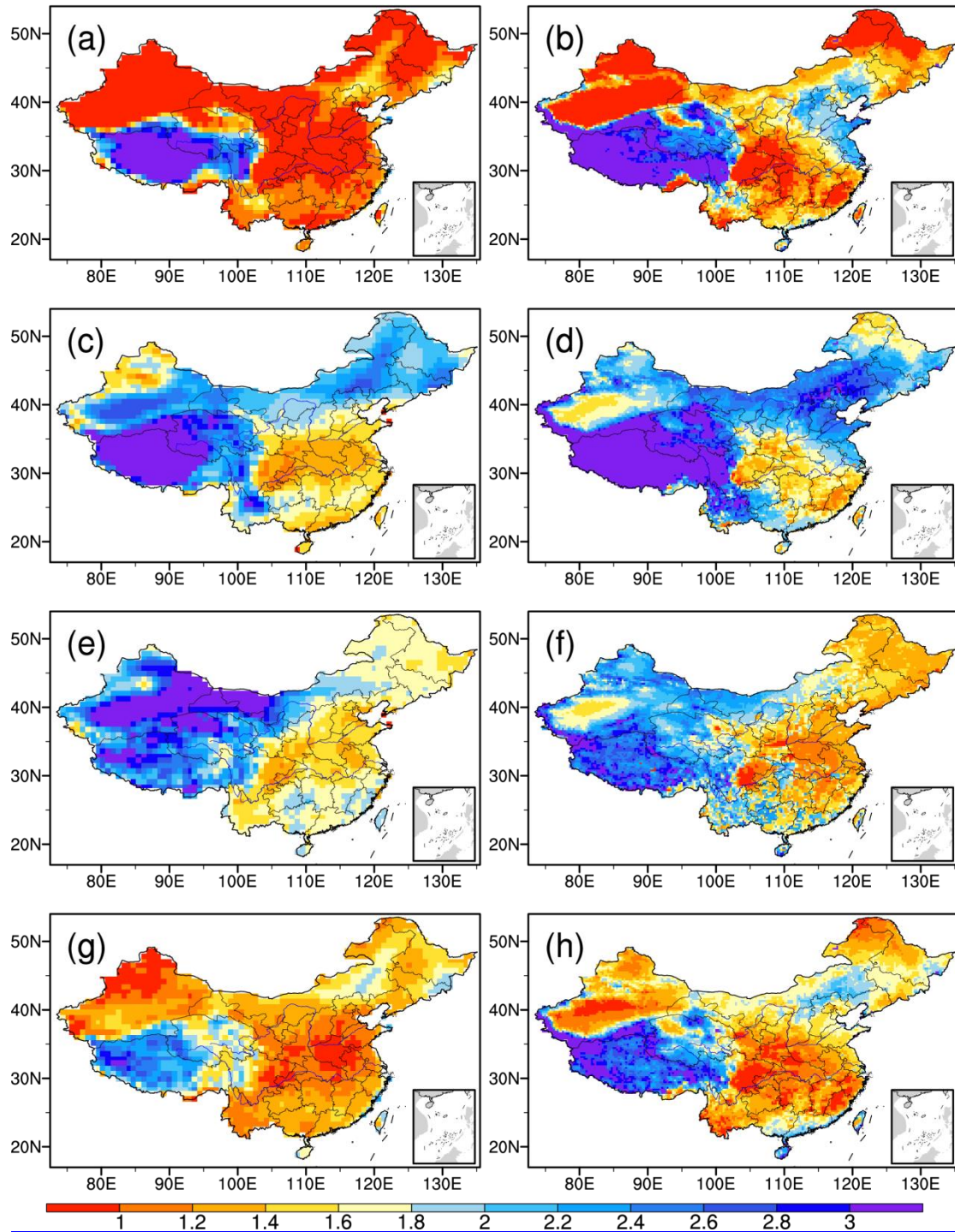


**Figure 2.** Spatial distribution of seasonal AEC (unit:  $10^4 \text{t/a/km}$ ) during 1986-2005: (a-b) winter, (c-d) spring, (e-f) summer, (g-h) autumn. Left panel is for the observation and the right panel is for the ensemble simulation.



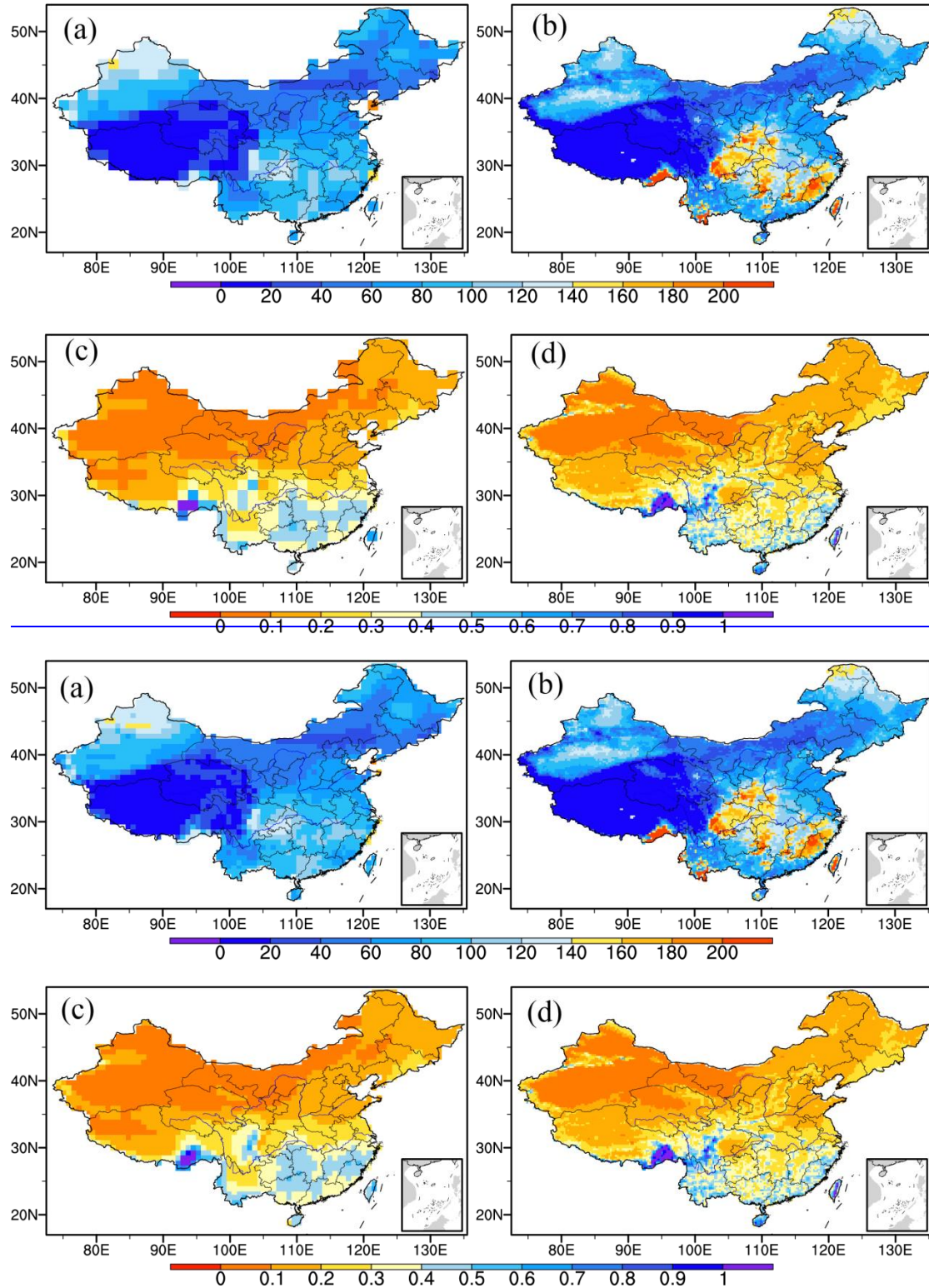


**Figure 3.** Spatial distribution of (a-b) the number of weak ventilation days per year and (c-d) wet deposition (unit:  $10^4 \text{ t/a/km}$ ) during 1986-2005: (a, c) observation, (b, d) ensemble simulation.

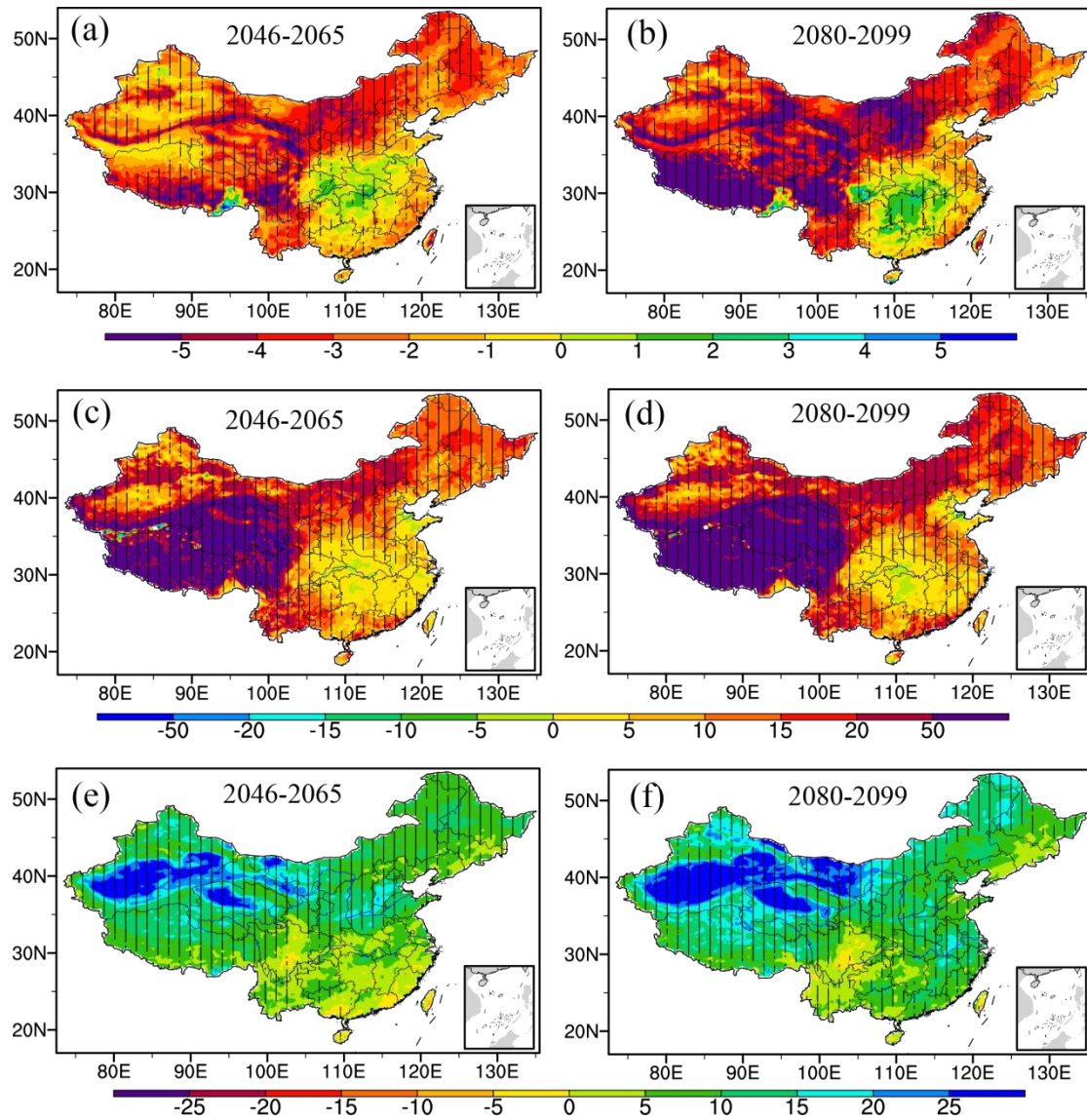


**Figure 4.** Ensemble projected percentage changes (relative to 1986-2005) in (a-b) AEC, (c-d) WVD, and (e-f) wet deposition during 2046-2065 (left panel) and 2080-2099 (right panel). Hatched regions indicate all ensemble members agree on the sign of change.

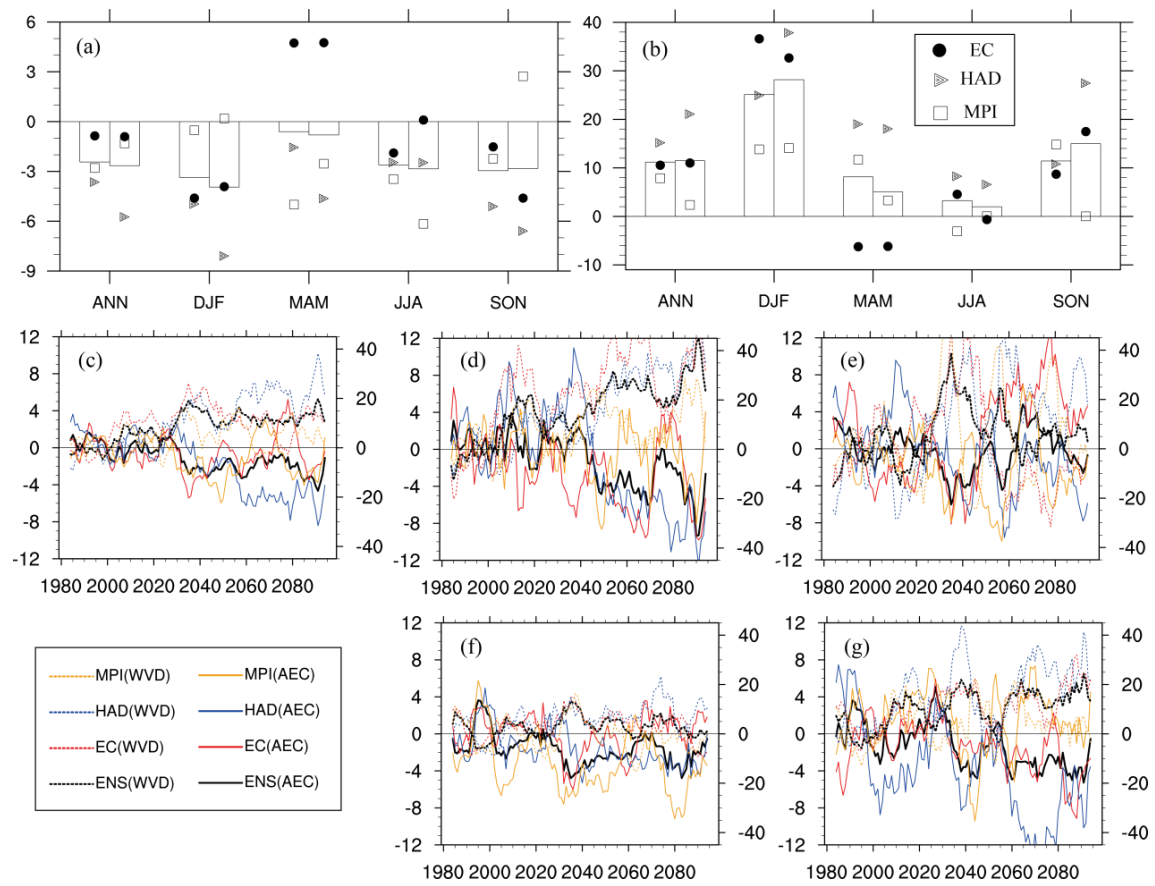


**Figure 5.** Range of projected percentage changes (relative to 1986-2005) in (a) AEC and (b) WVD during 2046-2065 and 2080-2099, and 9a running mean time series of percentage changes in (c) annual, (d) winter (DJF), (e) spring (MAM), (f) summer (JJA), (g) autumn (SON) for the Beijing-Tianjin-Hebei region. In Figure (a-b), the bars represent the ensemble projection and the marks represent the individual projection of the three members; the left (right) bar in each group is for 2046-2065 (2080-2099). In Figure (c-g), the solid (dashed) lines represent changes in AEC (WVD).

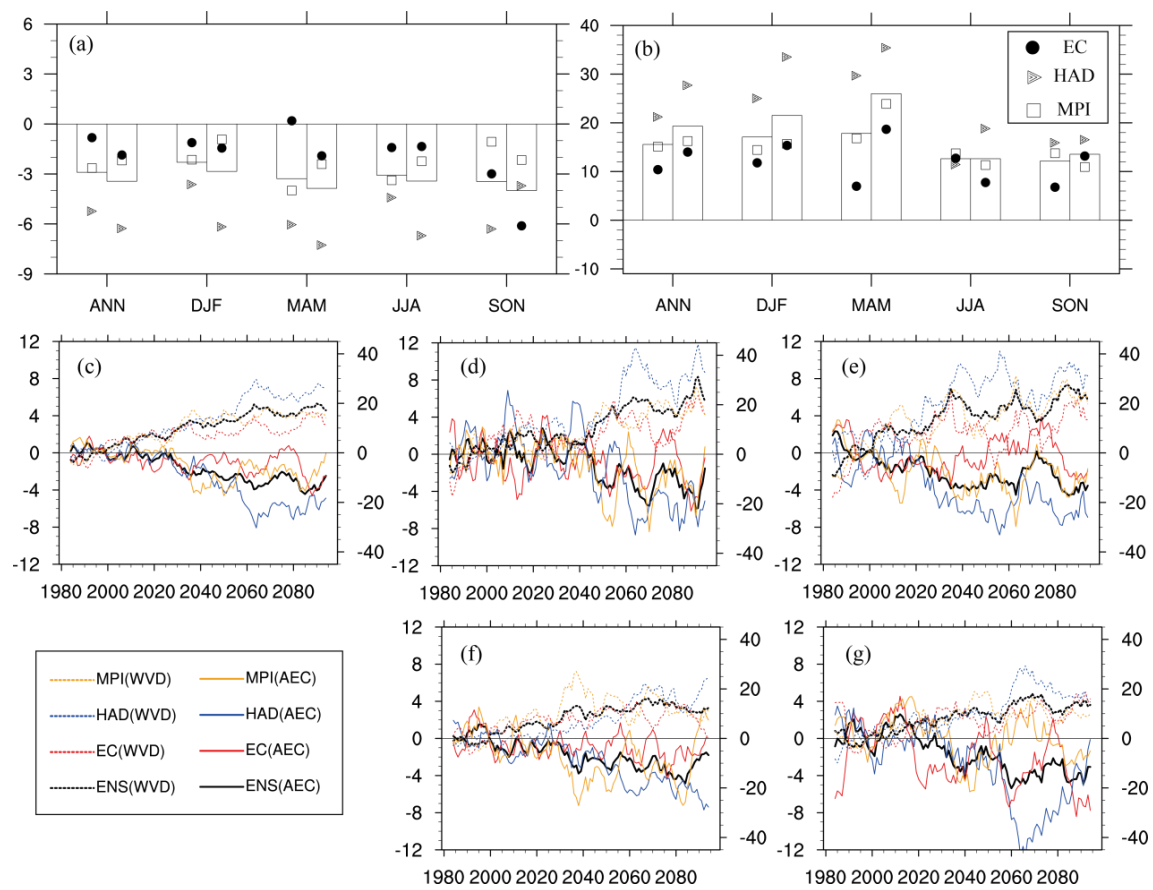


**Figure 6.** Same as Figure 5, but for Northeast China.

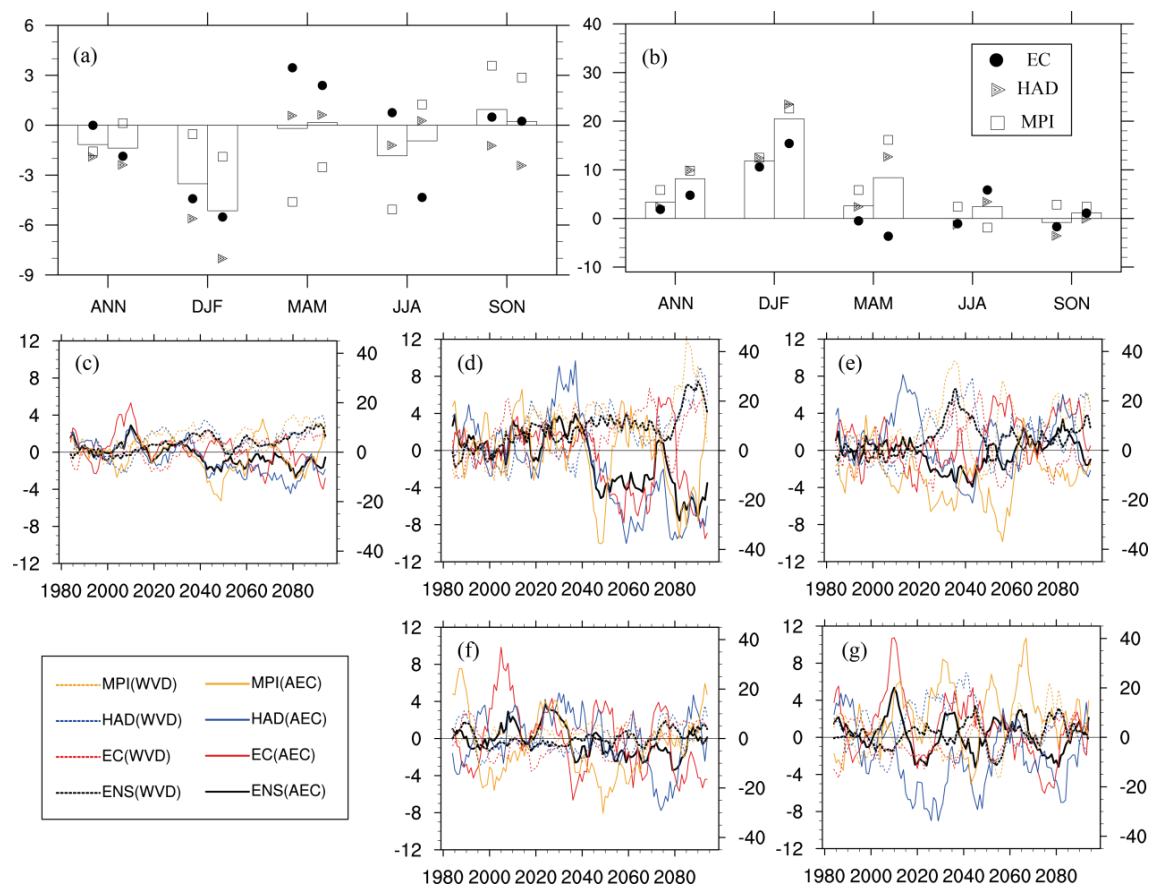


**Figure 7.** Same as Figure 5, but for Yangtze River Delta economic zone.



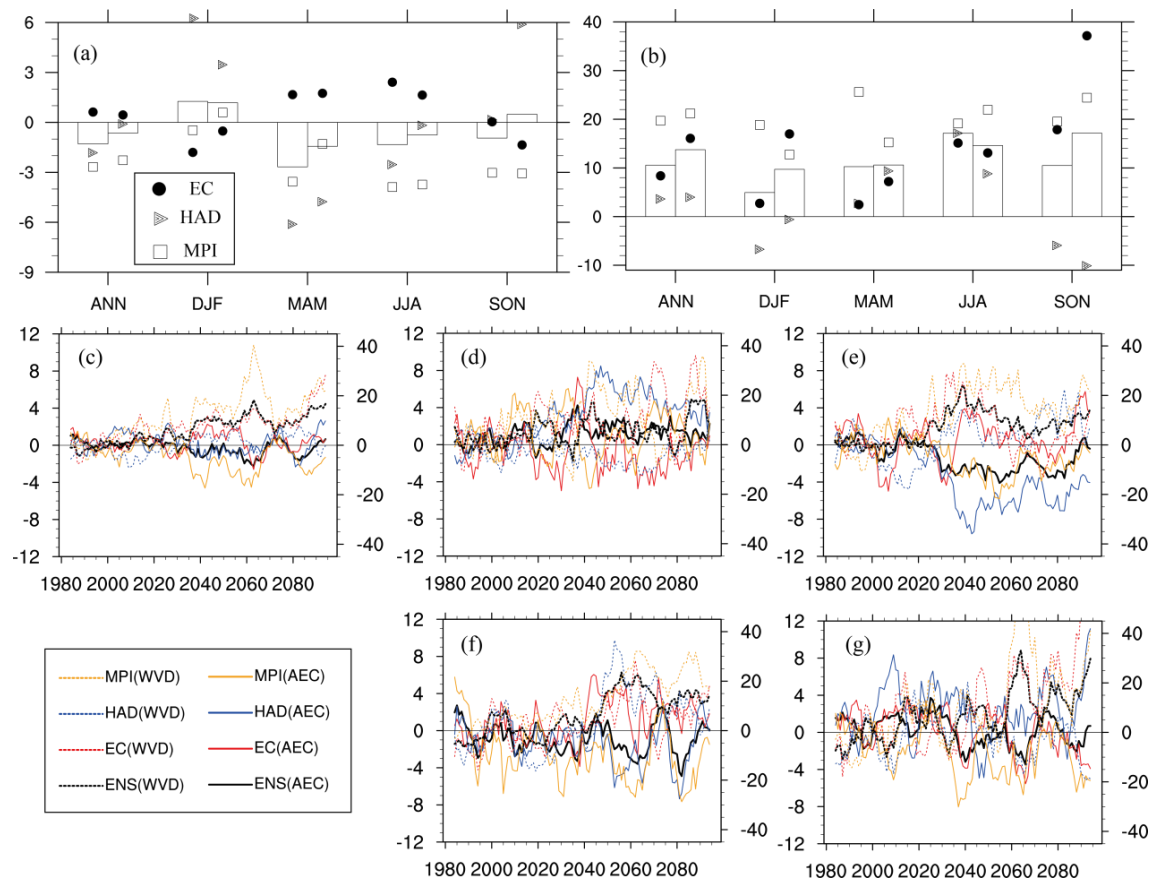


**Figure 8.** Same as Figure 5, but for Pearl River Delta economic zone.



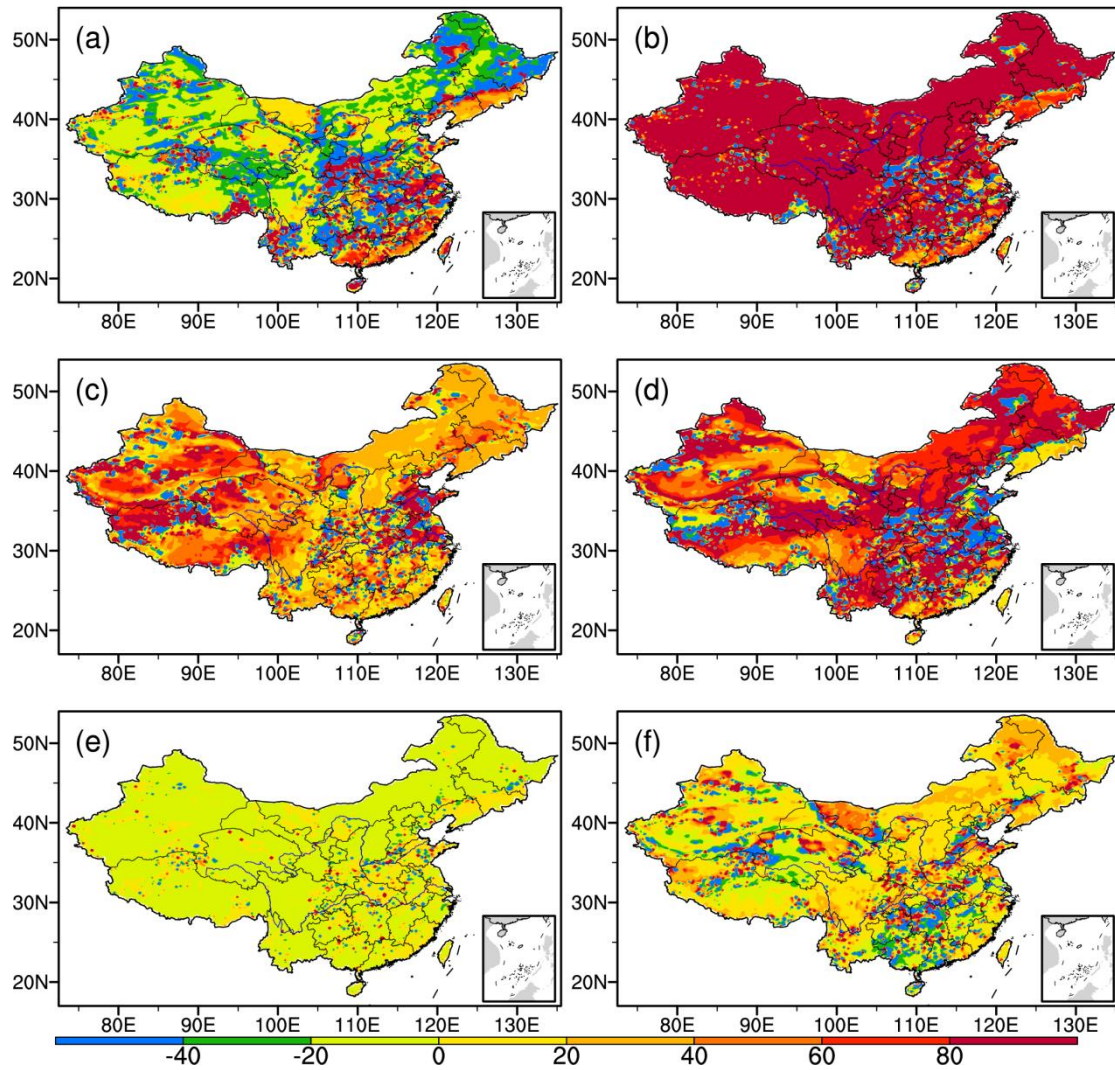


**Figure 9.** Relative contributions (unit: %) of individual components to annual AEC change in the middle of the 21st century based on the ensemble results. (a) precipitation, (b) ventilation, (c) wind speed averaged with the boundary layer, (d) boundary layer depth, (e) nonlinear term, (f) transient term.

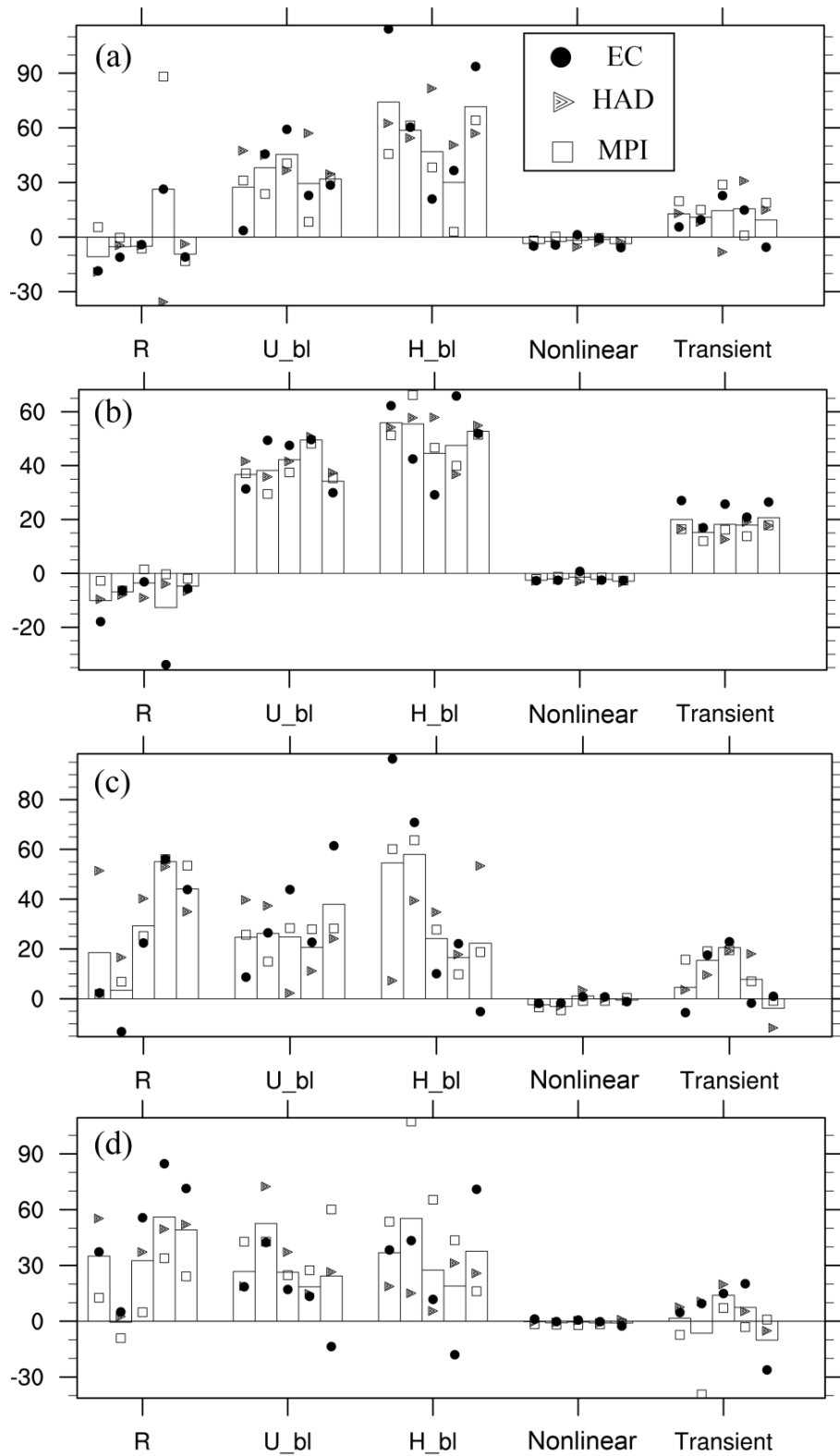


**Figure 10.** Relative contributions (unit: %) of individual components to annual AEC change in the middle of the 21st century averaged over four main economic zones of China: (a) BTH, (b) NEC, (c) YRD, (d) PRD. The bars represent the ensemble

710 projection and the marks represent the individual projection of the three members.

711 Bars from left to right in each group are in turn for annual, DJF, MAM, JJA, and

712 SON.